Many-objective optimization with improved shuffled frog leaping algorithm for inter-basin water transfers

Guo, Yuxue; Tian, Xin; Fang, Guohua; Xu, Yue Ping

DOI
10.1016/j.advwatres.2020.103531

Publication date
2020

Document Version
Accepted author manuscript

Published in
Advances in Water Resources

Citation (APA)
Guo, Y., Tian, X., Fang, G., & Xu, Y. P. (2020). Many-objective optimization with improved shuffled frog leaping algorithm for inter-basin water transfers. *Advances in Water Resources*, *138*, Article 103531. https://doi.org/10.1016/j.advwatres.2020.103531

Many-objective optimization with improved shuffled frog leaping algorithm for inter-basin water transfers

Yuxue Guo[1], Xin Tian[2], Guohua Fang[3], Yue-Ping Xu[1*]

[1] Institute of Hydrology and Water Resources, Civil Engineering and Architecture, Zhejiang University, Hangzhou, 310058, China

[2] Department of Water Management, Delft University of Technology, Delft, 2623CN, Netherlands

[3] College of Water Conservancy and Hydropower Engineering, Hohai University, Nanjing, 210098, China

[*]corresponding author. E-mail address: yuepingxu@zju.edu.cn

Highlights

- We propose a many-objective optimization methodology to water resources allocation for inter-basin water transfers.
- An improved shuffled frog leaping algorithm is developed to solve the many-objective optimization problem.
- The proposed algorithm performs well in the Eastern Route of South-to-North Water Transfer Project in Jiangsu, China.

Abstract: Inter-basin water transfers (IBWT) are implemented to re-allocate unevenly distributed water resources. However, many conflicting objectives associated with society, economy, and environment have made the water resources allocation problem in IBWT more complicated than ever before. Thus, there is a continuous need for in-depth research with the latest optimization techniques to secure many-objective allocation of water resources for IBWT. In addition, being troubled of easily falling into local minima and premature convergence in some multi-objective optimization algorithms, it is necessary to explore new alternatives to improve their search quality. Here we propose a many-objective optimization methodology for IBWT, which includes three modules: (1) formulating a many-objective optimization problem based on realistic controls; (2) developing a new multi-objective real-coded quantum inspired shuffled frog leaping algorithm (r-MQSFLA) to solve the optimization problem; (3) utilizing the Analytic Hierarchy Process (AHP)-Entropy method to filter the Pareto solutions. In r-MQSFLA, the real-coded quantum computer and the external archive with dynamic updating mechanism are applied to SFLA. The performance of r-MQSFLA is first compared to that of other multi-objective evolutionary algorithms (MOEAs) in solving mathematical benchmark problems. A case study of the Eastern Route of South-to-North Water Transfer Project in Jiangsu Province, China varying from a normal to an

extremely dry year, demonstrates that r-MQSFLA displays approximate performance on some compared algorithms and is improved significantly than MOSFLA in terms of convergence, diversity and reasonable solutions. This study can update the understanding of quantum theory to MOEAs and will provide a reference for better water resources allocation in IBWT under uncertainty.

Key words：Many-objective optimization; inter-basin water transfers; r-MQSFLA; AHP-Entropy method; Eastern Route of South-to-North Water Transfer Project

1 Introduction

Demand for water is relentlessly growing driven by industrial growth, irrigation, higher living standards and climate change. However, uneven distribution of water resources both in spatial and temporal scales is common in many countries, and thus results in water pressure and water shortage risks. The inter-basin water transfers (IBWT), referred to as the transfer of water from one geographically distinct river basin to another, or from one river reach to another, has been an effective engineering countermeasure to mitigate unevenly distributed water resources and balance the inter-basin water resource development (Akron et al., 2017; Zhou et al., 2017; Gallardo andAldridge, 2018). There are many IBWT projects such as the California State Water Project and the Central Utah Project in United States (Lopez, 2018), the Lesotho Highlands Water Project in Lesotho and South Africa (Matete andHassan, 2006), the West to East Water Transfer Project in Pakistan (Jeuland et al., 2019), and the Quebec Water Transfer Project in Canada (Lasserre, 2017). It is all known that China has planned and implemented many IBWT projects, one of which is the South-to-North Water Transfer (SNWT) Project (Yan andChen, 2013; Tang et al., 2014; Zhuang et al., 2019). After investing approximately $20 billion and resettling more than 300,000 people (Ministry of Water Resources, 2002), the SNWT project has become the largest and most expensive IBWT megaproject in the world (Pohlner, 2016).

The water resources allocation problem related with supply-oriented IBTW is very complicated not only under the conditions of the changing water demands, but also the complex water diversion works, construction of long tunnels, mass water pumping, sluice and reservoir operation. Furthermore, many conflicting objectives have made the water resources allocation problem more complicated than ever before (Vogel et al., 2015). For example, in some IBWTs conflict may arise from maximizing water supply reliability as opposed to minimizing the use of water resources or hydraulic structures; on the other hand, minimizing

costs rather than maximizing water demand may also be important in other IBWTs. Undoubtedly, water resources allocation of IBWT would be operated from a regional scale concentrating in one objective by a central planner to an inter-basin scale balancing social, economics, and environmental concerns by different stakeholders. Accordingly, optimizing water allocation schemes between the supplying basin and the demanding basin is a crucial and challenging task. Multi-objective evolutionary algorithms (MOEAs) that using an iterative search process to modify and evolve a population of candidate solutions (Reed et al., 2013) can effectively solve complex system problems and thus can be considered as a promising way to provide intelligent water allocation strategies. There have been many studies using the state-of-the-art MOEAs to investigate the applicability and effectiveness of water allocation in an inter-basin scale (Nouiri, 2014; Zeff et al., 2014; Yong et al., 2015; Zhou et al., 2015; Zhou et al., 2017; Fang et al., 2018a).

According to the selection mechanisms, the MOEAs can be divided into three categories, namely Pareto-based method, Decomposition-based method, and Indicator-based method (Bai et al., 2019). The Pareto-based MOEAs rely on the Pareto dominance to identify high-quality solutions. Representations of these dominance-based approaches include Non-dominated Sorting Genetic Algorithm II (NSGA-II) (Deb et al., 2002), Strength Pareto Evolutionary Algorithm 2 (SPEA2) (Bleuler et al., 2001), and epsilon-MOEA (ε-MOEA) (Deb et al., 2005). The decomposition-based MOEAs transfer a multi-objective problem into multiple single-objective subproblems, each of which is then solved in a cooperative manner. MOEA/D (Zhang et al., 2009) and reference vector-guided EA (RVEA) (Cheng et al., 2016) are typical examples of this kind. The Indicator-based MOEAs exploit performance indicators to guide the evolution process, such as representative approaches based on the hypervolume indicator including Hypervolume Indicator-Based Evolutionary Algorithm (IBEA) (Zitzler andKünzli, 2004) and metric selection EMOA (SMS-EMOA) (Beume et al., 2007). However, some Pareto-based MOEAs perform invalidly when more objectives are involved; the approaches based on hypervolume prefer non-uniformly-distributed solutions on non-linear Pareto fronts, and the performance of MOEA/D is sensitive to the pre-defined weight vectors when decomposing the objective space (Yang et al., 2018). Overall, although some achievements have been obtained in the field of multi/many-objective optimization recently, MOEAs still have plenty of space to explore.

Like the other MOEAs, the Pareto-based multi-objective shuffled frog leaping algorithm (MOSFLA) has been widely applied to solve multi-objective optimization problems in many fields, such as reservoir flood control (Li et al., 2010), mobile robot path planning (Hidalgo-

Paniagua et al., 2015) and product transport (Lamboia et al., 2016). MOSFLA was developed based on SFLA which is one of the population-based EAs inspired by natural memetics with only a couple of parameters, fast calculation speed and excellent global search capability (Eusuff et al., 2006). However, SFLA can quickly fall into local minima and has slow convergence in the later stage of the evolution and poor calculation accuracy (Elbeltagi et al., 2007), and thus it is commonly coupled with other advanced algorithms to find global optimal solutions effectively (Orouji et al., 2013; Ahandani andAlavi-Rad, 2015). One of the crucial topics concentrates on the quantum-inspired SFLA (QSFLA) characterized by certain principles of quantum mechanisms for a typical computer, and QSFLA was successfully used for its fast convergence (Gao andCao, 2012; Wang et al., 2019). Since there is rarely any published work to deal with many-objective optimization problems using QSFLA based on the Pareto theory, we use a real-coded quantum computer and an external archive with dynamic updating mechanism to save and update the non-dominated solutions in the multi-objective r-QSFLA (r-MQSFLA). These are considered to not only efficiently improve the diversity and convergence of Pareto solutions for many-objective optimization problems, but apply the quantum theory to MOEAs.

In this study, we aim to optimize water allocation for IBWT by developing a new multi-objective algorithm r-MQSFLA to generate a number of candidates (Pareto solutions), from which stakeholders can then choose a desirable policy using multiple criteria decision-making (MCDM) methods. The performance of r-MQSFLA is first benchmarked on mathematical test problems by comparing its performance with that of NSGA-II, SPEA2, IBEA, ε-MOEA, MOEA/D and MOSFLA. Then an integrated methodology combining many-objective optimization model, r-MQSFLA, and MCDM to optimize water resources allocation for IBWT is performed on a case study of the Eastern route of SNWT Project in Jiangsu Province, China (JE-SNWT) under normal, dry, and extremely dry scenarios. This integrated methodology with r-MQSFLA can provide optimal solutions with preferred weights for decision makers who have diverse preferences with a number of high-order Pareto candidates.

2 Methodology

The proposed many-objective optimization methodology with r-MQSFLA is shown in **Fig. 1**. In this methodology, the many-objective optimization model to water resources allocation for IBWT aims to maximize the water resources benefits (e.g., social, economic and eco-environment) as much as possible while satisfying all kinds of constraints. The model operates by determining an optimal release for each reservoir/lake or pumpage for each

pumping station over the whole operation period. The objective function and associated constraints of the multi-objective optimization model for IBWT can be formulated as follows.

$$opt \ \ F(x) = \left\{ f_1(x), f_2(x), ..., f_n(x) \right\} \tag{1}$$

$$s.t \ x \in G(x) \tag{2}$$

where $F(x)$ is objective function set; $f_n(x)$ is the objective function considering maximum social, economic and eco-environmental benefits; n is the number of the objective function; x is the decision variable; $G(x)$ is the constraint sets.

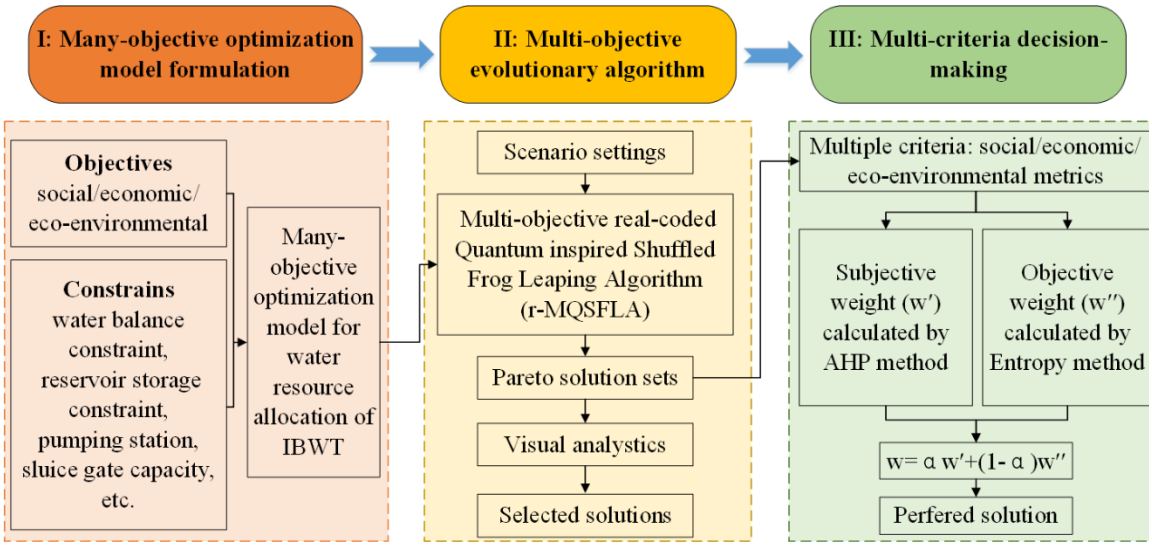

Fig. 1. Many-objective optimization methodology for water resources allocation of IWBT.

2.1 MOSFLA

Shuffled frog leaping algorithm (SFLA) is a meta-heuristic optimization method inspired from the memetic evolution of a group of frogs cooperating to look for food (Liu et al., 2019). It consists of a set of frogs divided into different groups referred to as memeplexes (sub-populations). Within each memeplex, the individual frog holds ideas that can be influenced by the ideas of other frogs, and these ideas can evolve through a process of memetic evolution. MOSFLA is a Pareto-based MOEA of the original SFLA executing three stages (Hidalgo-Paniagua et al., 2015). The first stage is to initialize both the variables and the initial population. The second stage consists of sorting the initial population according to the individual fitness and crowding distance and then dividing it into many sub-populations. In the last stage, the evolution of individuals is made per each sub-population. When all the iteration numbers in the sub-populations have been reached, the whole population is mixed

and then sorted again according to the Pareto front ranking and crowding distance. In this way, a set of non-dominated frogs will be made through the whole generation.

2.2 r-MQSFLA

2.2.1 r-QSFLA

Quantum-inspired shuffled frog leaping algorithm (QSFLA) is based on the concepts of qubits and superposition of states of quantum mechanics. The smallest unit of information stored in a two-state quantum computer is called a qubit. A qubit may be in the '1' state ($|1\rangle$), in the '0' state ($|0\rangle$), or in any superposition of the two (Kirar andAgrawal, 2019). The state of a qubit can be represented by Eq.(3).

$$|\psi\rangle = \alpha|0\rangle + \beta|1\rangle \tag{3}$$

where α and β are the probability amplitudes of the corresponding states, α^2 gives the probability that the qubit will be found in the "0" state and β^2 gives the probability that the qubit will be found in the "1" state, following constraint, $|\alpha|^2 + |\beta|^2 = 1$.

QSFLA is a multi-agent optimization system inspired by social behaviour metaphor of a quantum frog. Each agent, called a quantum frog, shuffles and leaps in a *D*-dimensional space according to the historical experiences of its own and its colleagues. There are *h* quantum frogs in a quantum frog colony that is in a space of *D* dimensions. The position of the quantum frog colony is $V = (v_1, v_2, ..., v_h)$. The i^{th} quantum frog's quantum position is $v_i = (v_{i1}, v_{i2}, ..., v_{iD})$, and a quantum position can be defined as a string of quantum bits.

$$v_{id} = \left[\begin{array}{c|c|c|c} \alpha_{id,1} & \alpha_{id,2} & \ldots & \alpha_{id,m} \\ \beta_{id,1} & \beta_{id,2} & \ldots & \beta_{id,m} \end{array}\right] \tag{4}$$

where $|\alpha_{id}|^2 + |\beta_{id}|^2 = 1$, $d = 1, 2, ..., D$, $i = 1, 2, ..., h$, and *m* is the total numbers of a qubit.

After all the quantum frogs are encoded in qubits, the i^{th} quantum frog's quantum position is observed to generate the quantum frog $X_i = (x_{i1}, x_{i2}, ..., x_{iD})$. However, it is computationally complex to transform the quantum position to the real quantum variable in QSFLA. Our study attempts to apply the probabilistic representation of a real-coded quantum computer to SFLA to improve its global search ability. A frog population initialized by the quantum computer is implemented to overcome the shortcoming of the uneven distribution of the initial population in SFLA, while an adaptive strategy for the change of the quantum angle

is adopted to modify the quantum rotation gate, named as real-coded quantum inspired shuffled frog leaping algorithm (r-QSFLA).

A qubit can be represented here to replace $v=[\alpha,\beta]^T$ as $v=[\cos(\theta),\sin(\theta)]^T$, where $\cos^2\theta+\sin^2\theta=1$, $\theta\in[0,2\pi)$. Then, the d^{th} quantum position of the i^{th} quantum frog would be defined as an m-qubit shown below.

$$v_{id}=\begin{bmatrix}\cos(\theta_{id,1})&\cos(\theta_{id,2})&\dots&\cos(\theta_{id,m})\\ \sin(\theta_{id,1})&\sin(\theta_{id,2})&\dots&\sin(\theta_{id,m})\end{bmatrix} \tag{5}$$

Instead of evaluating the position as a binary code, a real two-dimensional variable value of the d^{th} quantum frog representation is generated using Eq. (6). The two-dimensional transfer function was firstly implemented in Quantum Differential Evolution (QDE) algorithm by Chen et al. (2013). Its effectiveness was verified in QDE algorithm using the function

$$\begin{bmatrix}x_{id}^0\\ X_{id}^1\end{bmatrix}=\begin{bmatrix}\frac{b_d-a_d}{2}&0\\ 0&\frac{b_d-a_d}{2}\end{bmatrix}\begin{bmatrix}\cos(\theta_{id,1})&\cos(\theta_{id,2})&\dots&\cos(\theta_{id,m})\\ \sin(\theta_{id,1})&\sin(\theta_{id,2})&\dots&\sin(\theta_{id,m})\end{bmatrix}+\begin{bmatrix}\frac{b_d+a_d}{2}\\ \frac{b_d+a_d}{2}\end{bmatrix} \tag{6}$$

extreme value and traveling salesman problems compared with GA and PSO algorithm.

where $X_{id}\in[a_d,b_d]$, a_d is the lower bound of the d^{th} dimensional variable and b_d is the upper bound of the d^{th} dimensional variable.

The d^{th} position of the local worst quantum frog v_w is updated by using the rotation gate (Arpaia et al., 2011), shown in Eq. (7).

$$v_w=\begin{bmatrix}\cos(\Delta\theta)&-\sin(\Delta\theta)\\ \sin(\Delta\theta)&\cos(\Delta\theta)\end{bmatrix}v_w \tag{7}$$

Here, we apply two methods to modify the rotation gate, a self-adapting change strategy of the quantum angle $\Delta\theta$ and a self-correction of quantum position v.

a. The small value of θ causes low diversity while the big one hinders the algorithm convergence. To lessen this impact, we propose an adaptive strategy for the change of the quantum angle $\Delta\theta$, as shown in Eq. (8).

$$\Delta\theta=\theta_{\min}+f(\theta_{\max}-\theta_{\min})rand\exp(\frac{N_{\text{gen}}}{N_{\text{maxgen}}}) \tag{8}$$

$$f=\frac{1}{\mathrm{M}}\sum_{m=1}^{M}\left|\frac{fit_{\text{best},m}-fit_{i,m}}{fit_{\text{best},m}}\right| \tag{9}$$

where $\theta_{\min}$ is the lower bound of the quantum angle and $\theta_{\max}$ is the upper bound of the quantum angle, $fit_{i,m}$ is the fitness value of the i^{th} frog on objective m, $fit_{best,m}$ is the global best fitness value for objective m, N_{gen} is the present iteration times, M is the number of objectives, and N_{maxgen} is the times of maximum iteration.

b. Moreover, the quantum position easily approaching 0 or 1 in the later stage of the algorithm leads to a local convergence. To avoid this, $v=\left[\cos(\theta)\ \sin(\theta)\right]^T$ reupdated by Eq.(10) has been successfully used in quantum generic algorithm (QGA) (Wang et al., 2016; Fang et al., 2018b). We also adopt this action here.

$$v=\begin{cases}\left[\sqrt{1-\varpi}\ \ \sqrt{\varpi}\right]^T & if\ |\cos(\theta)|^2\geq 1-\varpi \text{ and} |\sin(\theta)|^2\leq\varpi \\ \left[\sqrt{\varpi}\ \ \sqrt{1-\varpi}\right]^T & if\ |\cos(\theta)|^2\leq\varpi \text{ and } |\sin(\theta)|^2\geq 1-\varpi \\ \left[\cos(\theta)\ \ \sin(\theta)\right]^T & if\ |\cos(\theta)|^2\geq\varpi \text{ and } |\sin(\theta)|^2\leq 1-\varpi\end{cases} \tag{10}$$

where ϖ is a random variable ranging from 0 to 1. We assume ϖ=0.01 in this study.

2.2.2 External archive with dynamic updating mechanism

In this study, we use an external archive (ExA) with dynamic updating mechanism to save and update the non-dominated solutions obtained from the multi-objective algorithm (Modiri-Delshad andRahim, 2016). The dynamic updating mechanism consists of two primary operations, namely the simulated binary crossover (SBX) method and the dynamic crowding distance calculation.

The SBX is a real-coded crossover which is inspired by the single-point crossover used in binary-coded. In a SBX operator, two parent individuals cross to generate new individuals, as shown in Eq.(11). It can be used to increase the number of individuals if there are not enough individuals in ExA.

$$\begin{aligned} x_{1k}&=\frac{1}{2}\left[\left(1-\beta_k\right)p_{1k}+\left(1+\beta_k\right)p_{2k}\right] \\ x_{2k}&=\frac{1}{2}\left[\left(1+\beta_k\right)p_{1k}+\left(1-\beta_k\right)p_{2k}\right]\end{aligned} \tag{11}$$

where x_{ik} is the k^{th} variable of the i^{th} individual, p_{ik} is the i^{th} variable of parent individuals, and β_k is a random coefficient of the k^{th} variable, shown as follows.

$$\beta_k = \begin{cases} (2u)^{\frac{1}{1+\eta_c}} & u \le 0.5 \\ \left[\frac{1}{2(1-u)}\right]^{\frac{1}{1+\eta_c}} & u>0.5 \end{cases} \quad (12)$$

where u is a random number, $u \in (0,1)$, and η_c is the cross-distribution index, $\eta_c \ge 0$.

The crowding distance can measure the density around a solution in the Pareto front distribution. A solution with a larger crowding distance is located at a less crowded region, which will result in better diversity in the population. Accordingly, solutions to its two neighbors with a shorter crowding distance will be removed when ExA overloads (Xiang andZhou, 2015). The crowding distance for the i^{th} solution of the Pareto front can be calculated from Eq. (13).

$$D_i = \sum_{k=1}^{M} \left(\left| f_{k,i+1} - f_{k,i-1} \right| \right) \quad (13)$$

where D_i is the crowding distance of the i^{th} solution with its two closest neighbours, $f_{k,i+1}$ and $f_{k,i-1}$ are the k^{th} objective function of the $(i+1)^{th}$ and $(i-1)^{th}$ solution, respectively, and M is the number of objective functions, $k = 1, 2, ..., M$.

2.2.3 r-MQSFLA

We propose a multi-objective algorithm referred to as multi-objective real-coded quantum inspired shuffled frog leaping algorithm (r-MQSFLA) by combining the r-QSFLA and ExA with dynamic updating mechanism, which is shown in **Fig. 2**. The main processes of r-MQSFLA are as follows.

Step 1. Define objective function and specify parameters of the algorithm. The parameters used in r-MQSFLA include size of global population (N_{pop}), number of local population (N_l), size of local population (N_{lpop}), dimension of optimization problem ($N_{\dim}$), maximum number of generation for global population in each run ($N_{\max gen}$), maximum number of generation for local population in each run (N_{lmaxgen}), maximum number of model simulations (N_{sim}), and maximum number of the external archive (N_{ExA}).

Step 2. Initialize the position of the quantum frog colony V , and from V generate the real quantum frog colony X using the two-dimensional transfer function described in Eq.(6). Then measure every individual of the entire quantum frog colony X .

Step 3. Sort the population according to the Pareto front ranking and the non-dominated solution set is placed at front, followed by the dominated solution set. Divide it into many sub-populations and then save the non-dominated solutions in a temporary set (*ND)*.

Step 4. Update the ExA based on dynamic updating mechanism.

a. Mix up the non-dominated solutions in the *ND* with those in the ExA. Sort the new solution sets according to the Pareto front ranking and save the new non-dominated solutions in the ExA.

b. Check the numbers of the non-dominated sets, N_{nds}, in the ExA. If $N_{\text{nds}} > N_{\text{ExA}}$, perform step c; otherwise, increase the number of individuals to meet the defined requirements in ExA using the SBX method, and perform Step 4.

c. Compute the crowding distance of each solution for the non-dominated sets, and remove solutions with the smallest crowding distance. An infinite distance value is assigned to the boundary solution.

Step 5. Perform global exploration and local exploration by the r-QSFLA and SBX operator.

a. Randomly select a solution from ExA, and tag it as a good solution X_g .

b. Divide the entire colony into many sub-populations by the shuffled method based on Eq.(14).

$$j = \mathrm{mod}\left(i, N_l\right) \tag{14}$$

where the i^{th} frog is selected into the j^{th} sub-population.

c. For each sub-population, tag the first solution as a good solution $\boldsymbol{X}_b$ and the last solution as a bad solution $\boldsymbol{X}_w$. Thus, the quantum position of $\boldsymbol{X}_b$ is referred as one good position $\boldsymbol{V}_b$ and the position of $\boldsymbol{X}_w$ is referred as one bad position $\boldsymbol{V}_w$.

d. Update V_w based on the improved quantum gate $G\left(\theta\right)$ with V_b using Eq.(7), and generate X_w by a new position V_w . Compare the new solutions X_w with X_b , and define the updated solutions (X_w) using Eq. (15).

$$X_w = \begin{cases} \text{new } X_w & if \text{ new } X_w \text{ dominates } X_w \\ X_w & if \text{ new } X_w \text{ does not dominate } X_w \end{cases} \quad (15)$$

e. Save the new X_w. Alternatively, repeat Steps d-e with X_g, and save or generate a new X_w.

f. Perform analogue binary crossover and then sort the sub-population according to the Pareto front ranking. Repeat steps c-e until the pre-defined maximum iteration N_{lmaxgen} is reached.

g. Shuffle the sub-population to the new quantum frog colony *X* after the local searches are accomplished in all sub-populations.

h. Sort the newly formed frog colony according to the Pareto front ranking and divide it into sub-populations again and then save the non-dominated solutions in the *ND*. Repeat Steps 3-5 until the predetermined condition is satisfied.

Step 6. Export the optimal Pareto solutions.

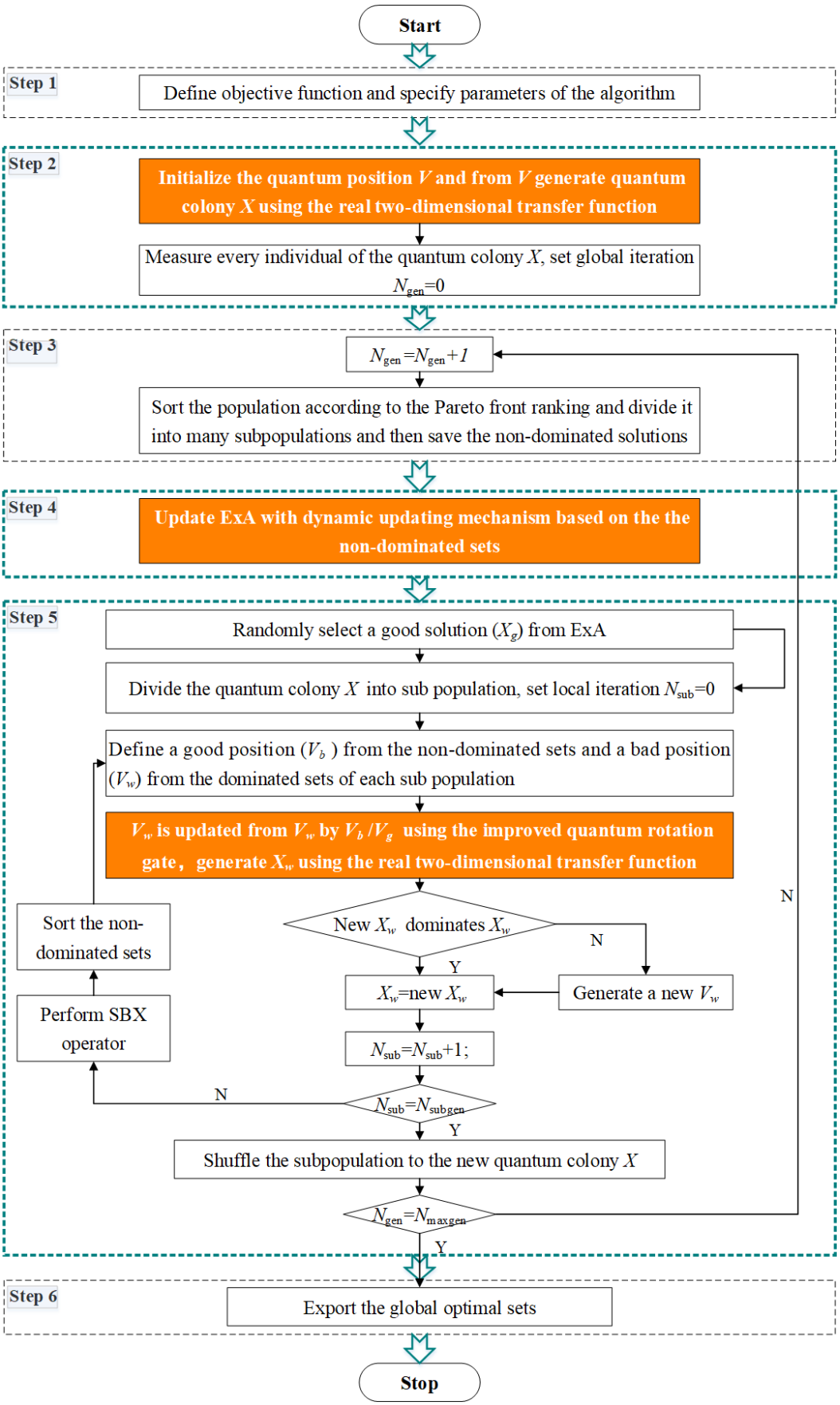

Fig. 2. Schematic diagram of the r-MQSFLA.

2.3 Pareto solutions filtered using AHP-Entropy method

After Pareto solutions are obtained from the optimization, the stakeholders of IBWT need to address the many-objectives that conflict with each other to determine preferred options. There are two widely methods for filtering Pareto solutions in water resources management, i.e., visual analytic approach (Kollat et al., 2011; Kasprzyk et al., 2012; Reed andKollat, 2013) and multiple criteria decision-making (MCDM) method (Madani andLund, 2011; Yang et al., 2016; Tian et al., 2019). Compared with the visual analytic approach, the MCDM method is less time-consuming in determining the preferred solution. In our case, we will implement the MCDM method to weight the objectives to seek operating options for IBWT. There are many evaluation methods in the field of MCDM, e.g., Analytic Hierarchy Process (AHP) (Chen et al., 2015), Entropy (Ridolfi et al., 2016), and TOPSIS (Zahmatkesh et al., 2015), which can be classified into three categories according to the weighting determining ways: subjective method, objective method, and combined subjective and objective method.

AHP is one of widely subjective analysis methods using a combination of qualitative and quantitative analysis, which is based on the knowledge and experience of experts and the intentions and preferences of decision-makers determining the index weight sorting. AHP has high reliability, profound mathematical background and can be applied to water resources (Aşchilean et al., 2017), agriculture (Ren et al., 2019) and renewable energy development (Ghimire andKim, 2018), etc. Entropy is an objective weight method depending on the impact of the relative change degree of the index on the system by calculating the information entropy of index. The greater the relative change degree of the index, the higher a weight it will be (Al-Aomar, 2010). To avoid the one-sided decision, the AHP method and Entropy method are coupled here to seek a comprehensive solution and to satisfy different decision makers. The evaluation step of the AHP-Entropy method (Wang et al., 2017) is as follows.

(1) Establish a hierarchical decision model.

Assuming that the number of evaluation indicators is *m* (here refers to objectives as indicators in MCDM) and Pareto solution sets is *n*, the options corresponding to evaluation indicators constitute the target decision matrix $Z = \left(z_{ij} \right)_{n \times m}$.

(2) Standardize data.

A decision matrix can be obtained after standardization which can be represented as $Y = (y_{ij})_{n \times m}$.

a. The standardization of "positive" indicator (the bigger, the better),

$$y_{ij} = \frac{z_{ij} - \min z_{ij}}{\max z_{ij} - \min z_{ij}} \tag{16}$$

b. The standardization of "reverse" indicator (the smaller, the better),

$$y_{ij} = \frac{\max z_{ij} - z_{ij}}{\max z_{ij} - \min z_{ij}} \tag{17}$$

(3) Apply the AHP method to derive subjective weights w' for quantitative criteria where the decision-makers can establish full pairwise preference. In AHP, by analyzing the relationship between various factors in the system, the evaluation indictors will be scored according to a nine-scoring system (Hua andLing, 2010) and described in a judgment matrix. Then, the subjective weight of each evaluation indictor can be attained by weight calculation and random consistency test based on the judgment matrix. This research is based on a project launched by the Department of Water Resources of Jiangsu Province. Therefore, we collected the score for each performance indicator according to the advice and guidance of government managers.

(4) Apply the Entropy method to derive objective weights w'' of quantitative criteria where decision preferences cannot be established.

(5) Apply a combined AHP-Entropy module for assessing criteria weights w of quantitative criteria where partial decision preference can be established using Eq. (18).

$$w = \alpha w' + (1-\alpha) w'' \tag{18}$$

where α is a weight of the subjective results relative to the objective, $\alpha \in (0,1)$.

(6) Define the preferred solution from the Pareto solutions with the maximum value of f_{topval} using Eq. (19).

$$f_{topval} = Y \times w \tag{19}$$

3 Case study: JE-SNWT Project

3.1 Study area

The SNWT aims to change the uneven spatial distribution of water resources in China by bringing water from the Yangtze River to the Hai, Yellow (Huang) and Huai River basins in North China. The project has three routes, namely western, middle and eastern routes, among which the middle and eastern ones have been in operation since 2014 and 2013, respectively, while the western one is still in planning. This study focuses on the eastern route of SNWT Project in Jiangsu Province (JE-SNWT), which is located between 32°15'-34°30' N and 117°00'-119°45' E, as presented in **Fig. 3**. Water from the Yangtze River is pumped by

pumping stations and then flows along the Grand Canal in Jiangsu Province, through a tunnel under the Yellow River and down an aqueduct to reservoirs in Shandong Province. The total area of the case study is about 62,000 km^2, and the total length of the main canals is about 404 km. This project consists of two canals (West Canal and East Canal), three lakes (Hongze (HZ) Lake, Luoma (LM) Lake and Nansi (NS) Lake) and eighteen pumping stations (Baoying, Jiangdu, etc.). The West Canal includes Bulao River, Xuhong River, and Jinbao Channel River, while the East Canal consists of Hanzhuang River, Zhongyun River, and Liyun River. The features of the pumping stations and sluices in the JE-SNWT Project are listed in **Table 1**. The three lakes have a total water storage capacity of about 45.3×10^8 m^3, whose storage characters are presented in **Table 2**.

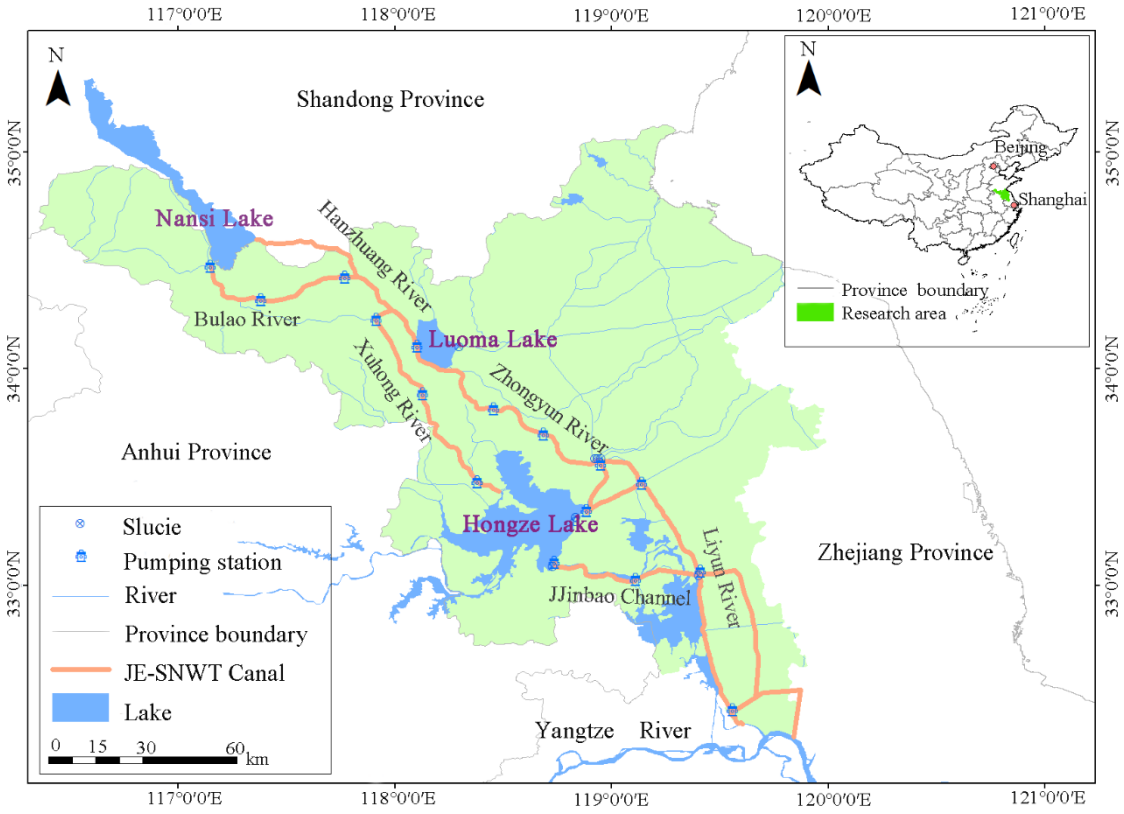

Fig. 3. Location of the JE-SNWT Project.

Table 1. Features of the pumping stations and sluices in the JE-SNWT Project.

	Location	Number	Capacity (m^3/s)		Location	Number	Capacity (m^3/s)
Pumping station	Baoying	P1	100	Pumping station	Liulaojian	P10	230
	Jiangdu	P2	400		Pizhou	P11	100
	Jinhu	P3	400		Zaohe	P12	175
	Huaian	P4	300		Taierzhuang	P13	125
	Hongze	P5	150		Liushan	P14	125

	Huaiyin	P6	300		Wannianzha	P15	125
	Sihong	P7	120		Xietai	P16	125
	Siyang	P8	230		Hanzhuang	P17	125
	Suining	P9	110		Linjiaba	P18	75
	Huaiyin	S1	500		Erhe	S4	500
Sluice	Yanhe	S2	500	Sluice	Gaoliangjian	S5	500
	Yangzhuang	S3	500		Nanyunxi	S6	400

Table 2. Features of the lakes in the JE-SNWT Project.

Lake	Dead water level (m)	Normal water level (m)		Regulation storage (10^8m^3)		Monthly minimum lake level for water diversion (m)			
		Flood season	Non-flood season	Flood season	Non-flood season	Apr. - Jun.	Jul.- Aug.	Sep. - Dec.	Nov. - Mar.
HZ	11.30	12.50	13.50	15.30	31.35	12.20	12.00	11.95	12.25
LM	21.00	22.50	23.00	4.30	5.90	22.60	22.15	22.15	22.55
NS	31.30	32.30	32.80	4.94	8.00	32.30	31.80	31.70	32.35

3.2 Water demands

According to the flow duration curve of the annual natural inflow data for 60 years, three hydrological years with an exceedance probability of 50%, 75% and 95% are selected to represent normal (1971.6-1972.5, annual mean inflow: $250.43\times10^8m^3$), dry (1958.6-1959.5, annual mean inflow: $134.72\times10^8m^3$), and extremely dry (1959.6-1960.5, annual mean inflow: $8.68\times10^8m^3$) scenarios, respectively. To provide the inputs associated with water demands for modelling water allocation under the three scenarios, the JE-SNWT Project is schematized and shown in **Fig. 4**.

In our case, water users can be categorized into 16 groups based on their locations. The water demands of water-supplying basins are related mainly to domestic, agricultural, and industrial, shipping, and ecological sectors. According to Chinese Standard (GB/T 51051-2014), the Water Quota Method is used to calculate the water demands for domestic, agriculture, and industrial sectors by integrating water quotas and activity levels with reuse rates and loss rates. The feasibility evaluation report of E-SNWT Project offers the shipping and ecological water demands. Year 2010 is selected as the base year for the designed scenarios in this study because no inter-basin water transfer project was implemented in this year, and scenarios are designed for 2030. **Fig. 5** shows the annual water demands of each water user in 2030 under (a) normal, (b) dry, and (c) extremely dry scenario, respectively. The water demands of the domestic, and industrial, shipping, and ecological sectors are the same under three scenarios, while the water demands of the agriculture sector increase with the hydrological probability. A total water demands of 127.73, 143.02, and $179.90\times10^8m^3$ can be

observed under normal, dry, and extremely dry scenarios, respectively, where the water demands of the agricultural sector is 65.37, 80.66, and 117.54 $\times 10^8 m^3$. It's noticed that the water demands of the agriculture sector is the largest in most water users. LYG User has the greatest demand for water, especially for the agricultural sector, followed by LM User and NS User. Regarding to the water demands for SD and AH user, we assume a specific value of 14.62 $\times 10^8 m^3$ and 0, respectively, based on the Planning Report of SNWT Project.

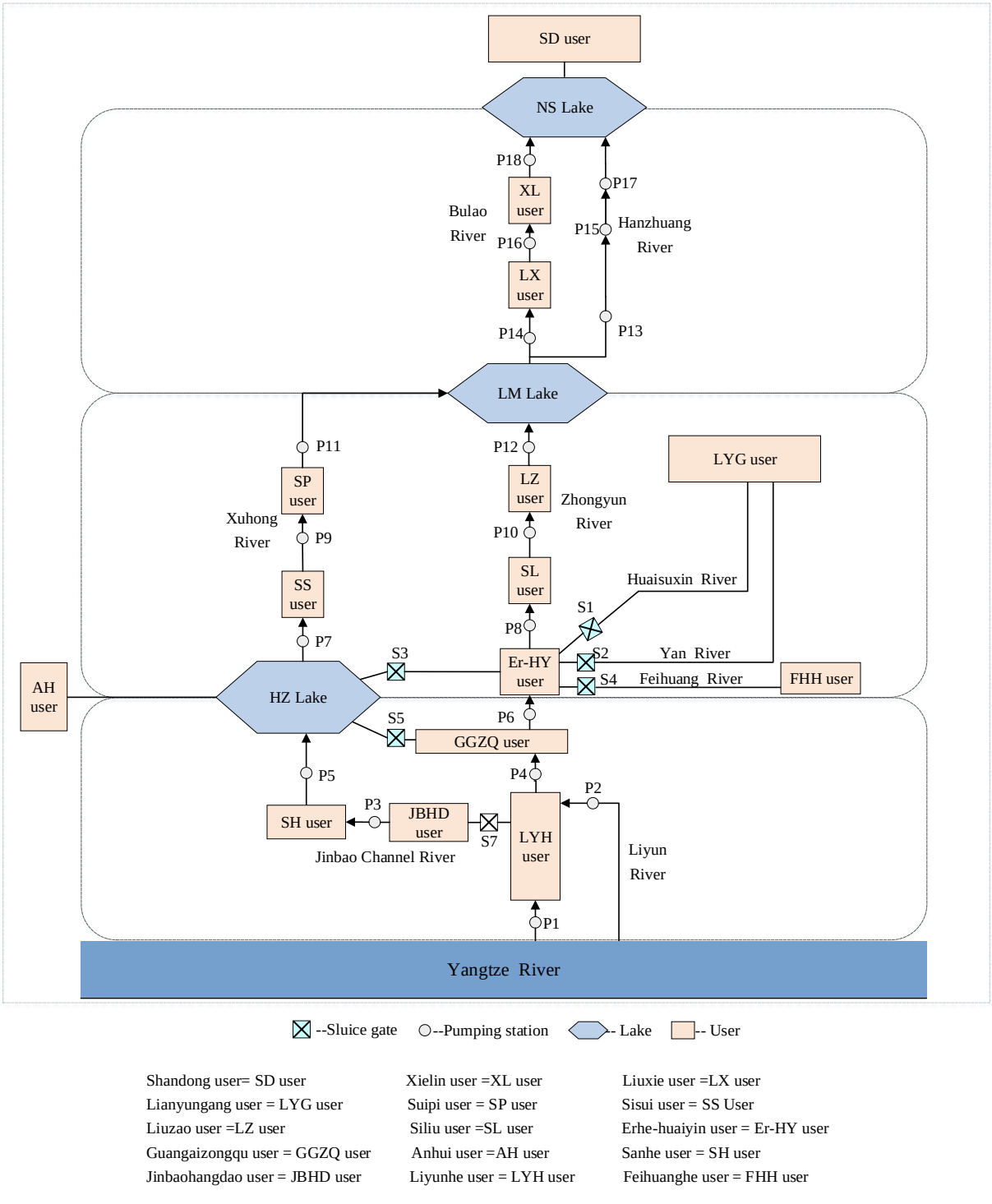

Fig. 4. Schematic diagram of the JE-SNWT Project.

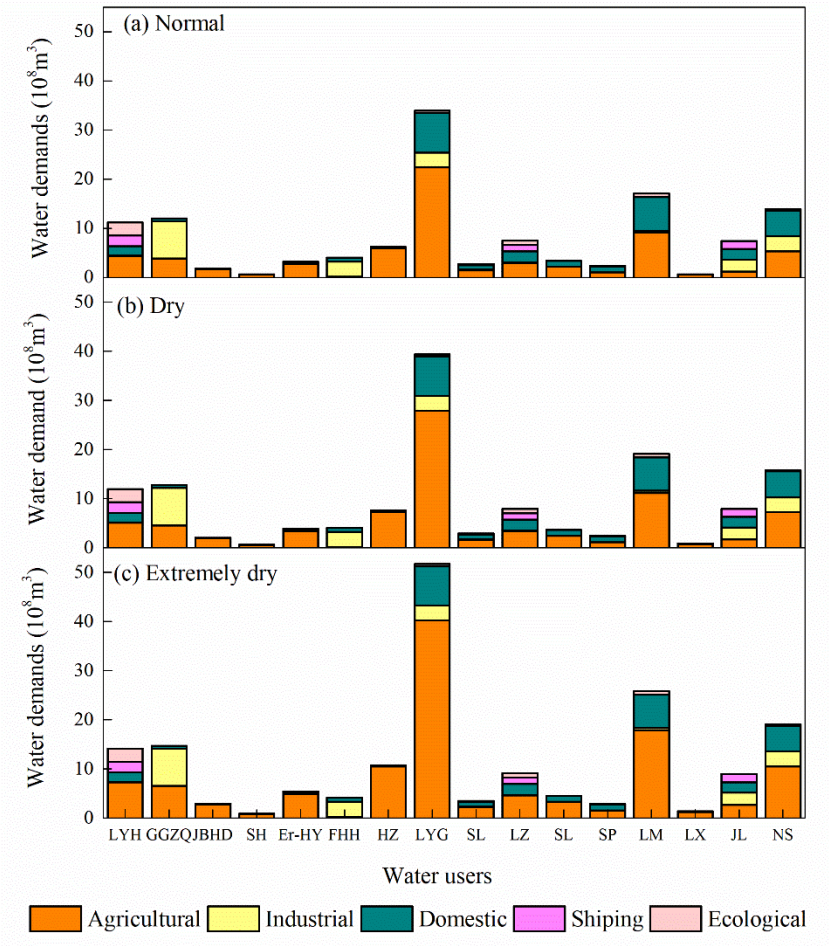

Fig. 5. Annual water demands of each water user in 2030 under (a) normal, (b) dry, and (c) extremely dry scenario.

3.3 Many-objective optimization problem formulation for the JE-SNWT Project

Herein, we formulate a five-objective optimization problem using a monthly time step for the JE-SNWT Project with 24 decision variables (18 pumping stations and 6 sluices). The objective function and associated constraints can be formulated as follows.

3.3.1 Objectives

(1) Minimizing the operating costs

A decision maker would consider a different suite of costs depending on whether an existing system is being managed or a completely new system is being designed. As water transfers occur in an existing system, costs considered in this study is the operating costs. The operating costs objective aims to minimize the costs for pumping stations operation here.

$$\min f_{\text{ocost}} = \sum_{t=1}^{T}\sum_{j=1}^{J} p_j q_{j,t}^{p} \Delta t \tag{20}$$

where p_j (RMB/m^3) is the operating cost of the j^{th} pumping station, $q_{j,t}^{p}$ (m^3/s) is water pumped by the j^{th} pumping station at time step t, $j=1,2,...,J$, J is the total number of pumping stations, $t=1,2,...,T$, T is the whole operating period, and Δt is the time step.

(2) Maximizing the water supply reliability

The water supply reliability metric is a measure of how well the water demand for users is met in a water transfer system. It gives the extent of water deficit and can be adopted as an indicator to reflect water supply efficiency for water demand.

$$\max f_{\text{wsrr}} = \left(1 - \frac{\sum_{t=1}^{T}\sum_{n=1}^{N} W_{n,t}^{s}}{\sum_{t=1}^{T}\sum_{n=1}^{N} W_{n,t}^{d}} \right) * 100\% \tag{21}$$

where $W_{n,t}^{s}$ (m^3) is the water deficit of the n^{th} user at time step t, $W_{n,t}^{d}$ (m^3) is the water demand of the n^{th} user at time step t, $n=1,2,...,N$ and N is the total numbers of the user, N=16.

(3) Minimizing the water surplus

Minimizing the amount of spill water, which can increase the amount of water to meet the water demand, is a widely used objective to evaluate water transfers systems operation performance.

$$\min f_{\text{wsv}} = \sum_{t=1}^{T}\sum_{m=1}^{M} W_{m,t}^{p} \tag{22}$$

where $W_{m,t}^{p}$ (m^3) is the water surplus of the m^{th} lake at time step t, $m=1,2,...,M$, and M is the total numbers of the lakes (M=3 in this case study).

(4) Minimizing the water withdrawn from the Yangtze River

Reducing the water withdrawn from the river aims to decrease the amount of water imported from the transfer system other than the inflow of lakes and improve the regulation and storage capacity of lake.

$$\min f_{\text{wrv}} = \sum_{t=1}^{T} W_{t}^{r} \tag{23}$$

where W_{t}^{r} (m^3) is the amount of water withdrawn from the river at time step t.

(5) Minimizing the lake storage deficit

Eq. (24) describes the ratio of the lake storage deficit at the end of a flood season. This objective seeks to maximize the lake storage at the end of a flood season, which potentially

reduces the amount of water transferred in the non-flood season and weakens the environmental impacts on water source basin.

$$\min f_{\text{ladr}} = 1 - \frac{\sum_{l=1}^{L} S_{l,f}}{\sum_{l=1}^{L} S_{l,\max}} * 100\% \tag{24}$$

where $S_{t,\max}$ (m^3) is the maximum storage of the l^{th} lake at the end of flood season, $S_{l,f}$ (m^3) is the ending storage of the l^{th} lake at the end of flood season.

3.3.2 Constraints

There are five main constraints, including water balance constraint, lake storage constraint, pumping station and sluice capacity, and minimum lake levels for water diversion.

a. Water balance constraint

The water balance constraint should be satisfied in the water transfer process.

$$S_{t+1} = S_t + (q_t^i + q_{j,t}^p - q_{j+1,t}^p - q_t^s - q_t^r) \times \Delta t \tag{25}$$

where S_t (m^3) is the initial water storage at the beginning of period *t*, S_{t+1} (m^3) is the ending water storage at the end of period *t*, q_t^i, q_t^s, q_t^r (m^3/s) are the inflow, water supply and release at time step t, respectively, $q_{j,t}^p$, $q_{j+1,t}^p$ (m^3/s) is the water pumped by the j^{th} and $(j+1)^{th}$ pumping station at time step t, respectively.

b. Lake storage constraint

$$S_{t,\min} < S_t < S_{t,\max} \tag{26}$$

where $S_{t,\min}$ and $S_{t,\max}$ (m^3) are the lower and upper storage boundary at time step t, respectively.

c. Pumping capacity constraint

$$0 \le q_t^p \le q_{t,\max}^p \tag{27}$$

where $q_{t,\max}^p$ (m^3/s) is the maximum pumping capacity at time step t.

d. Sluice capacity constraint

$$0 \le q_t^r \le q_{t,\max}^r \tag{28}$$

where $q_{t,\max}^r$ (m^3/s) is the maximum sluice capacity at time step t.

f. Minimum lake levels for water diversion

Water diverted will be stopped if the lake level is lower than the minimum level for water diversion. The monthly minimum lake level for water diversion is shown in **Table 2**.

4 Results

4.1 Mathematical benchmark test of r-MQSFLA

We first applied r-MQSFLA and six widely used MOEAs, namely NSGA-II, SPEA-II, ε-MOEA, IBEA, MOEA/D and MOSFLA, to solve five mathematical benchmark problems, ZDT1, ZDT2, ZDT3, ZDT4, and ZDT6 (Perolat et al., 2015). Specifically, NSGA-II, SPEA2, ε-MOEA, IBEA, and MOEA/D were performed in a MATLAB platform for evolutionary multi-objective optimization, PlatEMO (Tian et al., 2017b), and MOSFLA and r-MQSFLA were performed in MATLAB 2018b. The parameters for all MOEAs used in the benchmark problems are listed in **Table 3**.

Table 3. Parameter ranges/values for each MOEA used in the benchmark problems.

No	Parameters	Range/value	Algorithms
1	Maximum number of model simulations	10	All Algorithms
2	Size of global population	100	
3	Maximum number of iterations for global population	20000	
4	Dimension of optimization problem	2	
5	Number of the external archive	100	r-MQSFLA, NSGA-II, SPEA2, MOEA/D, ε-MOEA
6	Maximum number of iterations for local population	10	r-MQSFLA, MOSFLA
7	Number of local populations	10	r-MQSFLA, MOSFLA
8	Number of qubits	1	r-MQSFLA
9	ε-dominance	0.001-0.0075	ε-MOEA
10	Simulated Binary Crossover (SBX) rate	0.5-1.0	r-MQSFLA, NSGA-II, SPEA2, IBEA, ε-MOEA
11	Distribution index for crossover	10-100	r-MQSFLA, NSGA-II, SPEA2, IBEA, ε-MOEA
12	Crossover probability	0.75-0.9	NSGA-II, SPEA2, MOEA/D
13	Mutation probability	0.0-0.5	NSGA-II, SPEA2, IBEA, ε-MOEA, MOEA/D
14	Distribution index for mutation	10-100	NSGA-II, SPEA2, IBEA, ε-MOEA, MOEA/D

In the benchmark problems, we used the indicators of generational distance (Reed et al., 2013), entropy for diversity (Deb andJain, 2002), hypervolume (Deb et al., 2003), and epsilon (Zitzler et al., 2003) to evaluate the performance of all algorithms. Note that a smaller generational distance and epsilon, and a larger diversity and hypervolume indicate a better performance. At the same time, we applied the Wilcoxon rank-sum test (Perolat et al., 2015),

which is a non-parametric test, to perform comparisons for each benchmark problem between r-MQSFLA and other algorithms. It shows that MOSFLA performs the worst for the five benchmark problems. We then mainly compared the r-MQSFLA with the other five algorithms (NSGA-II, SPEA2, IBEA, ε-MOEA, and MOEA/D). The results are shown in **Fig. 6**. In ZDT1, r-MQSFLA demonstrates good hypervolume and epsilon measures. ε-MOEA performs the best in terms of generational distance but is the worst in terms of diversity. It can be seen that the six algorithms have very good convergence to the Pareto optimal front on ZDT2. For diversity, SPEA2, r-MQSFLA, and ε-MOEA are the best, followed by NSGA-II, MOEA/D, and IBEA. Except IBEA, the other five algorithms all have better hypervolume and epsilon values. r-MQSFLA has higher generational distance, and smaller diversity and epsilon measures than some algorithm on ZDT3, but has significant improvements in diversity values. In ZDT4, ε-MOEA is the best in terms of generational distance, but r-MQSFLA is better than the other five MOEAs in terms of diversity, hypervolume and epsilon among obtained solutions. It is also evident that the performance measures of r-MQSFLA on ZDT6 are good, particularly in terms of diversity. Thus, from the two-objective problems studied above, we can conclude that the r-MQSFLA produces good convergence and diversity.

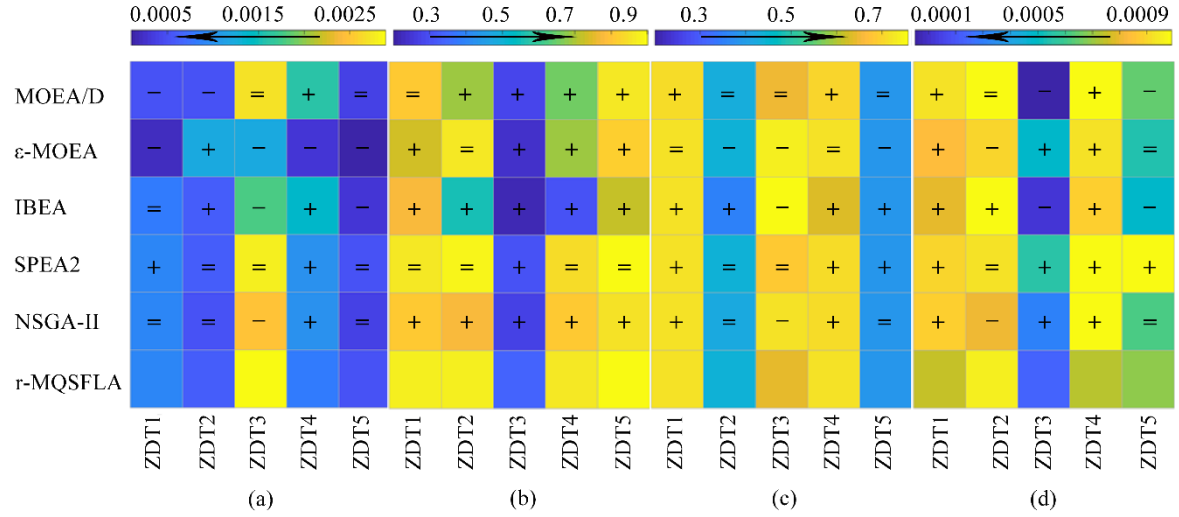

Fig. 6. Performance comparison of (a) generational distance, (b) diversity, (c) hypervolume, and (d) epsilon for the five mathematical benchmark problems using NSGA-II, SPEA-II, ε-MOEA, IBEA, MOEA/D and r-MQSFLA analyzed by the Wilcoxon rank-sum test. Three symbols of the Wilcoxon rank-sum test indicate the observation of the null hypothesis, with '+' indicating that the null hypothesis is rejected and r-MQSFLA displays statistically superior performance at the 95% significance level ($\alpha = 0.05$) on the compared algorithm; '−' indicating that the null hypothesis is rejected and r- MQSFLA displays statistically inferior performance at the 95% significance level on

the compared algorithm; '=' indicating that the null hypothesis is accepted and r-MQSFLA display approximate performance at the 95% significance level on the compared algorithm.

4.2 Many-objective optimization with r-MQSFLA for JE-SNWT Project

We then applied NSGA-II, SPEA2, IBEA, ε-MOEA, MOEA/D, MOSFLA and r-MQSFLA to solve the many-objective optimization problems for the JE-SNWT Project under normal, dry and extremely dry condtions. The parameters of maximum number of iterations for global population, dimension of optimization problem, and number of the external archive used in the case study are 2000, 5, and 500, respectively. The rest of the parameters are the same as those used in the benchmark problems. Unlike ZDT, where the analytical Pareto front is known, the JE-SNWT problems varying from a normal to an extremely dry year has unknown Pareto fronts. **Fig. 7** provides visualizations of the reference Pareto sets attained for these three problems across five runs of all of the MOEAs tested (NSGA-II, SPEA2, IBEA, ε-MOEA, MOEA/D, MOSFLA and r-MQSFLA). The geometries of the tradeoffs vary significantly across the applications, as would be expected given their different hydrological conditions. In each of the plots, the operating costs, water surplus, and water supply reliability are plotted on the x, y, and z axes, respectively. The color of the markers indicates the water withdrawn from the Yangtze River with color ranging from blue, representing low amount, to red, representing high amount. The lake storage deficit at the end of flood season is presented by the size of the makers, where the small marker means low deficit and the large one means high deficit. The black arrows have been added to guide the reader in understanding the directions of optimization. An ideal solution would be located at the bottom left corner (low operating costs, high water supply reliability, and low water surplus) of the plot and represented by a small (low lake storage deficit), dark blue (low water withdrawn from the Yangtze River) marker. The operating costs under all scenarios range from 0.62×10^{8} RMB to 6.91×10^{8} RMB. The water supply reliability has a positive relationship with natural inflow (positive relationship, i.e., the former increase with the increase of the latter). In contrast, the water withdrawn from the Yangtze River has an inverse relationship (inverse relationship, i.e., the former decrease with the increase of the latter) with natural inflow. The volume of water surplus under normal scenario varies in the range of 85.37×10^{8} m^3 to 133.85×10^{8} m^3, which is much higher than that under extremely dry scenario with a value of $0.00\times10^{8}m^3$ to $9.59\times10^{8}m^3$. Extremely dry scenario generates the widest range of the ratio of lake storage deficit at the end of the flood season while the other two scenarios have the similar smaller range.

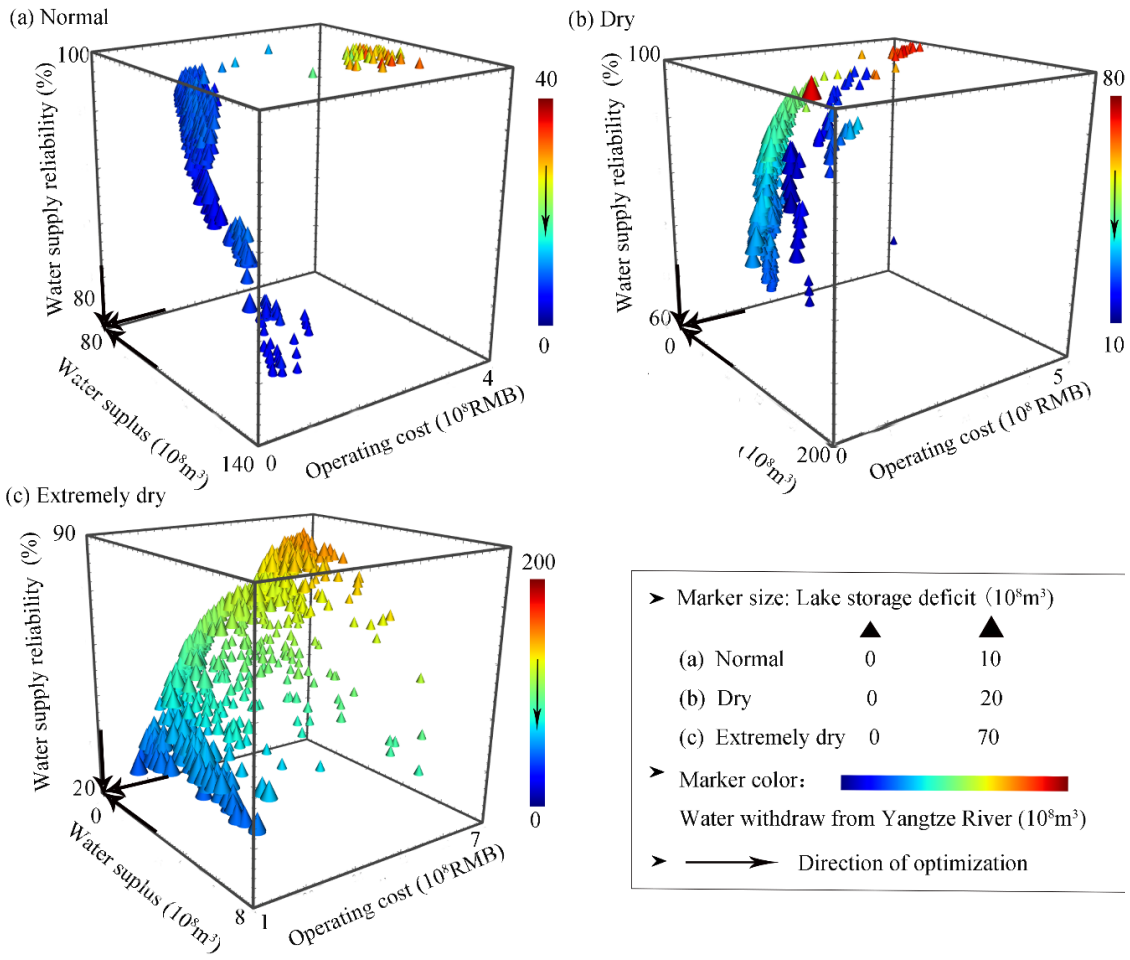

Fig. 7. Illustration of reference Pareto fronts attained across all runs of all algorithms for (a) normal, (b) dry, and (c) extremely dry scenario. The black arrow indicates the direction of optimization.

Fig. 8 (a), (c) and **(e)** provide the parallel reference Pareto sets with a total number of 1111, 1292, and 1263 solutions in the reference sets across the normal, dry, and extremely dry problems, respectively. All algorithms are presented with different colors. In terms of the percentage of the reference Pareto fronts captured by each MOEA, shown in **Fig. 8 (b), (d)** and **(f)**, r-MQSFLA (4.48%) and SPEA2 (3.79%) largely contribute to the reference sets for the normal condition; NSGA-II, SPEA2, ε-MOEA, and r-MQSFLA capture more compared with the remaining algorithms for both dry and extremely dry conditions. Although r-MQSFLA does not always perform the best in capturing the highest percent of the reference sets, it consistently captures a certain large percentage across all of the problems. MOSFLA is the worst-performing algorithm in terms of capturing reference set for the three applications, following by MOEA/D and IBEA. The latter two fail to capture any reference set under normal and dry conditions.

The black arrows in **Fig. 8** indicate the directions of optimization. An ideal solution would be a horizontal line intersecting the top of every vertical axis. However, the solutions with the greast operating costs incur large amounts of water surplus and water withdrawn from the Yangtze River while performing better in the water supply reliability and the lake storage deficit. For example, most solutions of r-MQSFLA and ε-MOEA overlap under normal and dry conditions and they prefer a position near the top values than SPEA2. These results imply that r-MQSFLA and ε-MOEA will generate higher operating costs and higher water withdrawn from the Yangtze River, but higher water supply reliability and lower lake storage deficit than SPEA2. It is interesting to note that r-MQSFLA has two distinct regions as reference Pareto front under normal and dry conditions, one of which has the largest operating costs and will widen the range of the reference sets. In addition, the geometries of the tradeoffs attained by r-MQSFLA, ε-MOEA, SPEA2 and NSGA-II vary significantly across the extremely condition. It is evident that r-MQSFLA captures the maximum operating costs (worst solutions) and maximum water supply reliability (best solutions). It is also worth noting that although most of the MOEAs tested are able to find portions of reference set under extremely condition, the problem is difficult with respect to finding well converged, consistent, and diverse solution sets by one MOEA.

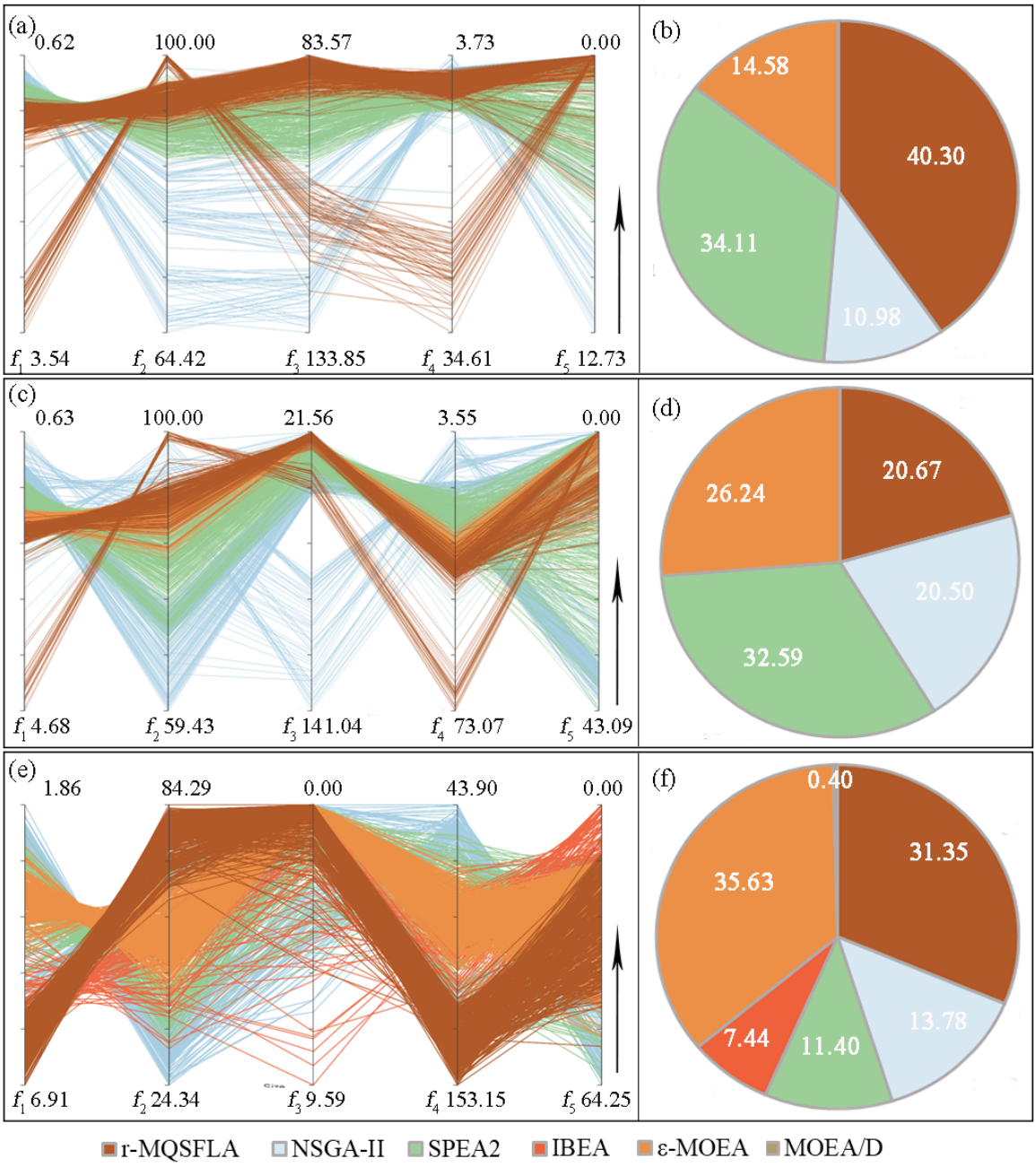

Fig. 8. Illustration of parallel reference Pareto sets attained across all runs of all algorithms for (a) normal, (c) dry, and (e) extremely dry scenario and percent contributions (%) across all runs of all algorithms for (b) normal, (d) dry, and (f) extremely dry scenario. f_1 represents operating costs (10^8RMB), f_2 represents water supply reliability (%), f_3 represents water surplus ($10^8 m^3$), f_4 represents water withdrawn from the Yangtze River ($10^8 m^3$), and f_5 represents lake storage deficit ($10^8 m^3$). The black arrow indicates the direction of optimization.

While capturing the reference set is important, it is necessary to evaluate each MOEA using the performance indicators. In the JE-SNWT problems, we also used the indicators of generational distance, diversity, hypervolume, and epsilon. The results are shown in Fig. 9. This table shows that there is no top performing algorithm in terms of the four indictors. For

example, for normal condition, r-MQSFLA has the best generation distance measures across all MOEAs, but performs worse than NSGA-II in diversity; for dry condition, r-MQSFLA obtains the worse hypervolume and epsilon distance than ε-MOEA, but shows better results in diversity; for extremely condition, r-MQSFLA achieves approximate values in epsilon distance and better values in diversity with ε-MOEA, but fails to obtain ideal results in generational distance. Over all, MOSFLA, IBEA, and MOEA/D are the weakest algorithms for all these three problems with larger generational distance and epsilon, lower diversity and hypervolume. The remaining algorithms have fairly consistent better run results, in particular while comparing r-MQSFLA with MOSFLA, which can satisfy one of our purposes, that is, improving MOSFLA in terms of convergence and diversity.

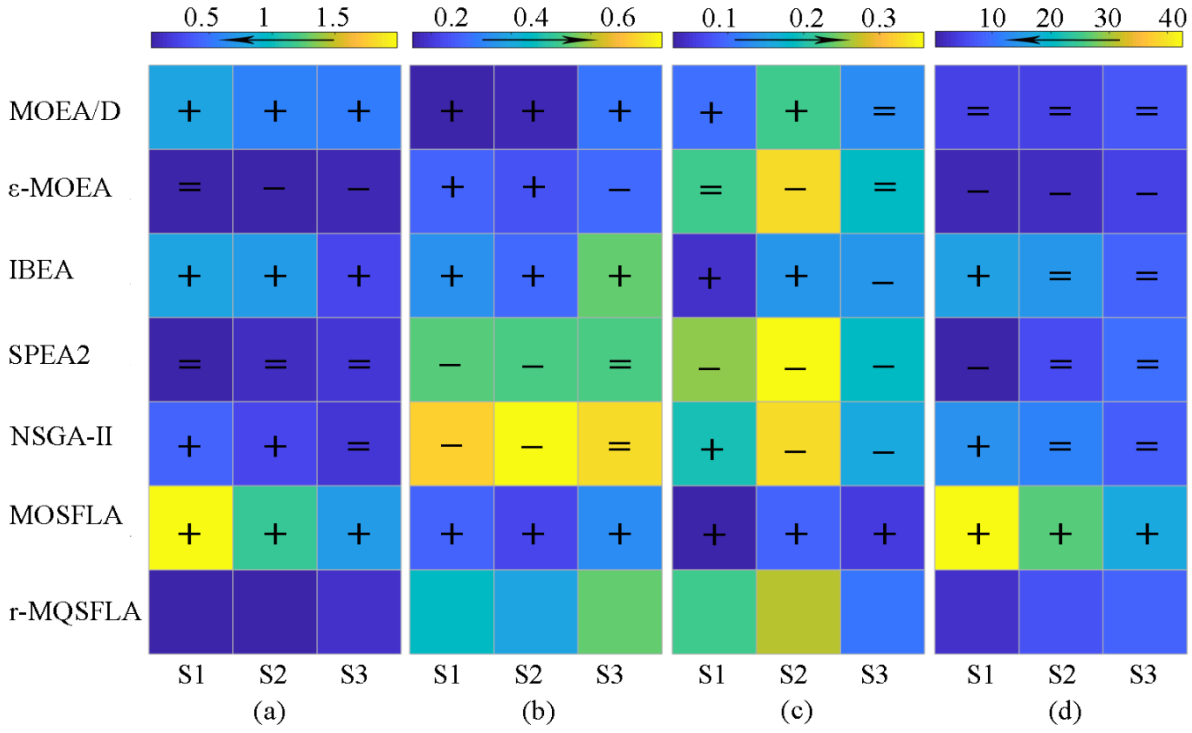

Fig. 9. Performance comparison of (a) generational distance, (b) diversity, (c) hypervolume, and (d) epsilon for the three JE-SNWT problems using NSGA-II, SPEA-II, ε-MOEA, IBEA, MOEA/D, MOSFLA and r-MQSFLA analyzed by the Wilcoxon rank-sum test. S1-3 represents the scenario of normal, dry, and extremely dry. Three symbols of the Wilcoxon rank-sum test indicate the observation of the null hypothesis, with '+' indicating that the null hypothesis is rejected and r-MQSFLA displays statistically superior performance at the 95% significance level ($\alpha = 0.05$) on the compared algorithm; '−' indicating that the null hypothesis is rejected and r- MQSFLA displays statistically inferior performance at the 95% significance level on the compared algorithm; '=' indicating that the null hypothesis is accepted and r-MQSFLA display approximate performance at the 95% significance level on the compared algorithm.

4.3 Pareto solutions filtered using AHP-Entropy method for JE-SNWT Project

The Pareto solutions are evaluated based on social, economic and eco-environment benefits. In our case, social benefits criteria include the performance metric of water supply reliability, economic benefits criteria include the performance metric of operating cost, the water withdrawn from the Yangtze River and water surplus, and eco-environment benefits criteria include the performance metric of lake storage deficit at the end of flood season. The water supply reliability is the "positive" evaluation indicator, while other performance metrics are the "reverse" evaluation indicators.

This study first applied the AHP method to calculate the subjective weights and then used the Pareto solutions to determine the objective weights based on the Entropy method. According to the government managers, the operating costs and water supply reliability are the two most striking metrics. Given that people prefer to make decisions based on losses rather than gains, the operating costs makes the top indictor under normal scenario, while water supply reliability has the largest contribution under the dry and extremely dry conditions. This could be reasonable assuming that the government aims for a sustainability-oriented policy, which may not be fully based on economic revenue, particularly in terms of severe conditions. An example is given with α=0.5 across all algorithms for the JE-SNWT Project under three scenarios, which is shown in **Table 4.** The water surplus has a minimal influence for all algorithms under extremely dry condition. This is because there is low inflow and not enough water to have a surplus.

Table 4. Criteria weights derived by the AHP-Entropy method for the JE-SNWT Project using NSGA-II, SPEA-II, ε-MOEA, IBEA, MOEA/D, MOSFLA and r-MQSFLA.

MOEA	Weight	Normal					Dry					Extremely dry				
		f_1	f_2	f_3	f_4	f_5	f_1	f_2	f_3	f_4	f_5	f_1	f_2	f_3	f_4	f_5
r-MQSFLA	w'	0.37	0.26	0.14	0.12	0.11	0.22	0.31	0.19	0.12	0.16	0.23	0.50	0.11	0.09	0.08
	w''	0.29	0.24	0.18	0.23	0.06	0.26	0.19	0.18	0.23	0.14	0.24	0.21	0.06	0.29	0.19
	w	0.33	0.25	0.16	0.17	0.08	0.24	0.25	0.18	0.17	0.15	0.24	0.36	0.08	0.19	0.13
MOSFLA	w''	0.27	0.17	0.26	0.29	0.01	0.27	0.27	0.20	0.24	0.02	0.24	0.22	0.16	0.25	0.14
	w	0.32	0.22	0.20	0.20	0.06	0.24	0.29	0.19	0.18	0.09	0.23	0.36	0.13	0.17	0.11
NSGA-II	w''	0.09	0.17	0.26	0.18	0.30	0.06	0.27	0.17	0.14	0.35	0.18	0.25	0.14	0.19	0.24
	w	0.23	0.22	0.20	0.15	0.20	0.14	0.29	0.18	0.13	0.25	0.21	0.37	0.12	0.14	0.16
SPEA2	w''	0.03	0.31	0.26	0.05	0.35	0.12	0.27	0.16	0.18	0.27	0.13	0.18	0.12	0.18	0.39
	w	0.20	0.29	0.20	0.08	0.23	0.17	0.29	0.17	0.15	0.21	0.18	0.34	0.11	0.13	0.23
IBEA	w''	0.29	0.28	0.17	0.26	0.00	0.22	0.36	0.22	0.19	0.00	0.13	0.20	0.07	0.21	0.39
	w	0.33	0.27	0.16	0.19	0.05	0.22	0.34	0.21	0.16	0.08	0.18	0.35	0.09	0.15	0.23
ε-MOEA	w''	0.24	0.26	0.21	0.09	0.21	0.18	0.25	0.08	0.22	0.27	0.16	0.23	0.03	0.20	0.39
	w	0.31	0.26	0.18	0.10	0.16	0.20	0.28	0.13	0.17	0.21	0.19	0.36	0.07	0.14	0.23

MOEA/D	*w*"	0.26	0.16	0.24	0.28	0.06	0.24	0.27	0.13	0.31	0.05	0.12	0.25	0.11	0.20	0.32
	w	0.32	0.21	0.19	0.20	0.08	0.23	0.29	0.16	0.22	0.10	0.17	0.37	0.11	0.15	0.20

Note: f_1 represents operating costs (10^8RMB), f_2 represents water supply reliability (%), f_3 represents water surplus (10^8m^3), f_4 represents water withdrawn from the Yangtze River (10^8m^3), and f_5 represents lake storage deficit (10^8m^3). *w*' represents the subjective weights, *w*" represents the objective weights, and *w* represents the combined weights.

Fig. 10 shows the variation of the six MOEAs relative to r-MQSFLA on the five metrics. For the metrics of water surplus and lake storage deficit, we only presented the absolute results of those more than zero obtained by some MOEAs. For example, SPEA2 can generate extra lake deficit with a value of 0.13 $\times 10^8 m^3$. Make the five metrics all be bigger the better, and consequently a good MOEA prefers a negative variation of the five metrics relative to other MOEAs. In this case, all metrics characterized by r-MQSFLA perform better than those characterized by SPEA2, MOEA/D, and MOSFLA for normal condition, and IBEA and MOSFLA for dry condition, demonstrating that r-MQSLA is able to reduce the operating costs while enhancing water supply reliability. In terms of extremely dry condition, r-MQSFLA chooses to sacrifice economic cost in exchange for water supply reliability, resulting in the increase in water withdrawn from the Yangtze River and lake storage deficit. However, as we mentioned that people prefer to make decisions based on losses rather than gains, this result obtained by r-MQSFLA may accord with the aspirations of both government and general public and is more reasonable. MOSFLA will generate water surplus even under tremendous drought condition. The result of that water surplus is zero, indicating that our proposed many-objective optimization methodology with r-MQSFLA can fulfill the water resource utilization to secure water supply.

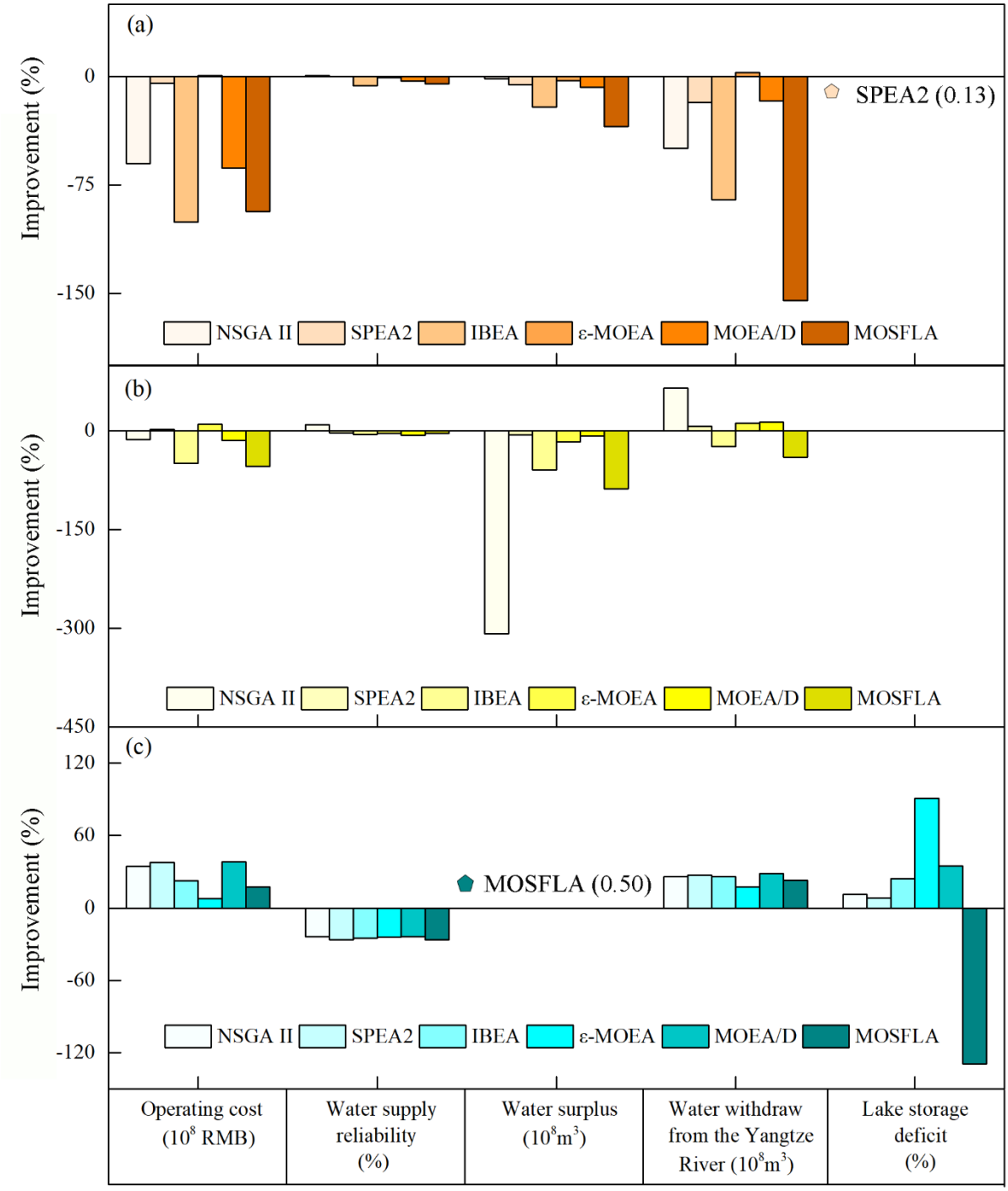

Fig. 10. Variation of the six MOEAs relative to r-MQSFLA on the five metrics for (a) normal, (b) dry, and (c) extremely dry scenario.

We further presented the comparison between annual water supply and water demands characterized by the preferred solutions with r-MQSFLA under three scenarios, as shown in **Fig. 11**. According to the guiding policy of Water Resources Department of Jiangsu Province, water supply through the JE-SNWT project is planned to satisfy water demands for domestic sector firstly, followed by industrial, shipping and ecological sectors, and the last one is

agricultural sector. Thus, the water demands for domestic sector are fully met under three scenarios, while that for industrial sector cannot be satisfied in case of extremely dry condition with a lack of $5.58\times10^8 m^3$. We find that water supply for shipping and ecological sectors can almost meet requirements under all hydrological conditions. However, the shortage of water supply for agricultural sector ranging from $4.45\times10^8 m^3$ to $60.51\times10^8 m^3$ is enlarged with the decreased natural inflow. This insufficiency is not caused by our many-objective optimization methodology with r-MQSFLA, but resulted from the limitation of the capacity of pumping stations, sluices, and reservoirs in JE-SNWT Project.

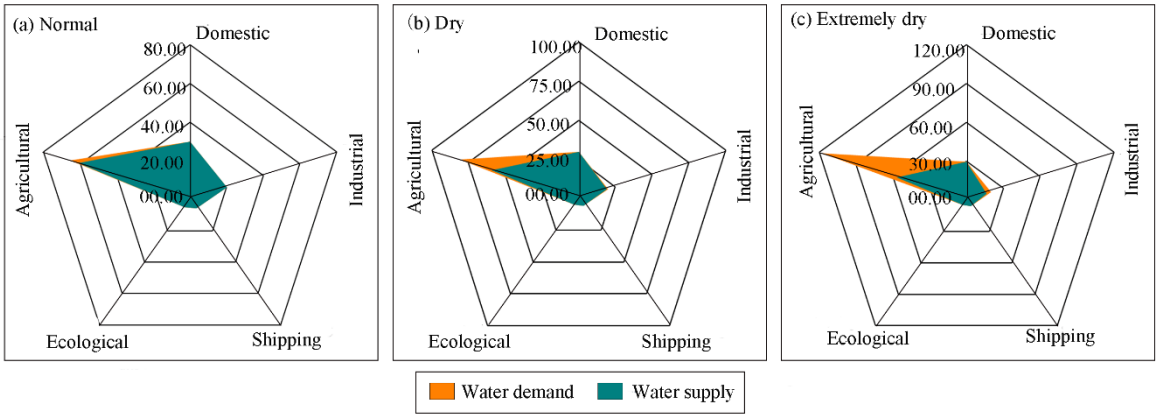

Fig. 11. Comparison between annual water supply and water demands under (a) normal, (b) dry, and (c) extremely dry scenario.

5 Discussion

5.1 Improving algorithm efficiency for many-objective optimization problems

Tools such as MOEAs are suitable to solve many-objective optimization problems in real-word which exhibit nonlinear, convex or non-convex, and with discontinuous or non-uniform distribution of the target space through the high-dimensional Pareto solutions (Kollat andReed, 2007). In addition, a branch of study on quantum-inspired EAs, for instance, QGA, quantum-inspired immune clonal particle swarm optimization algorithm, and quantum-inspired immune clonal algorithm, have demonstrated the feasibility and efficiency of the novel EAs based on the concept and principles of quantum computing (Jiao et al., 2008; Vlachogiannis andLee, 2008). This study proposed a new MOEA named as r-MQSFLA to generate a diverse set of non-dominated solutions for many-objective optimization problem.

The Multi-objective optimization algorithm aims to achieve two objectives: one is that the obtained non-dominated solution set should approach the real non-dominated solution set as quickly as possible, and the other one is that the solutions should be distributed as evenly as possible (Fonseca et al., 2003). The performance of r-MQSFLA was tested with that of

other MOEAs in solving five benchmark problems (ZDT1, ZDT2, ZDT3, ZDT4, and ZDT6). The indicator measures of convergence and diversity for the five benchmark problems indicate that r-MQSFLA inspired from a real-coded quantum computer can strength the search ability of SFLA, while the ExA with dynamic updating mechanism can improve the diversity of Pareto solutions.

In the case study, r-MQSFLA, SPEA2, ε-MOEA, and NSGA-II outperform the remaining algorithms in capturing the reference sets for all three problems. In particular, there are no Pareto solutions captured by the traditional MOSFLA. This result implies that the Pareto solutions of r-MQSFLA mostly dominating those of MOSFLA can facilitate higher water supply reliability with the same operating costs, which is critical to the decision makers in IBWT. The indicator measures of convergence and diversity argue that there is no top performing algorithm, but r-MQSFLA is improved significantly than MOSFLA. This further demonstrates that solutions updated by a rotation gate using an adaptive strategy of the quantum angle and a self-correction of quantum position in our study can successfully solve the local convergence of SFLA. In addition, from the comparison between the preferred solutions of r-MQSFLA and other MOEAs selected using AHP-Entropy, r-MQSFLA chooses to sacrifice economic cost in exchange for water supply reliability to get out of a tremendous drought condition. This result obtained by r-MQSFLA may accord with the aspirations of both government and general public and is more reasonable as people prefer to make decisions based on losses rather than gains. However, r-MQSFLA improves accuracy in solving complex many-objective optimization problems while sacrificing computational speed. r-MQSFLA is one time slower than MOSFLA for one simulation to perform one test problem.

5.2 Use of proposed approach for IBWT

Current optimization modelling of water transfer is operated based on economic measures and water demand. For example, Jain et al. (2005) analysed and designed a large IBWT system according to the water availability and demand in India. Sadegh et al. (2010) managed the inter-basin water resources based on the least-cost objective. Furthermore, Zhang et al. (2017) determined the amount of water transferred to maximize the water supply reliability involving the minimum water spillage. In addition to the least-cost and reliability objectives, there is still a need to add more pragmatic objectives in the water transfers process. Herein, we considered economic, social and environmental performance metrics together to

move beyond the general cost-reliability analysis by using volumetric metrics to measure the efficiency of water transfer, the utilization of natural inflow, and the influence on environment.

This study dealing with a five-objective optimization problem simultaneously solves 31 sub-problem (5 four-objective problems, 10 three-objective problems, 10 two-objective problems, and 5 single-objective problems). Many-objective visual analytics allows decision-makers to seek a compromise solution according to the trade-offs between objectives. However, it takes several steps starting from a two-dimensional to a three-dimensional trade-off to figure out the optimal solution. The AHP-Entropy method implemented in this study uses the quantitative objective metrics to directly explore the high-order Pareto sets. To avoid the subjective judge of the value of Pareto solutions, the subjective and objective weights are both considered to seek more comprehensive operating options for the water transfer managers. The AHP-Entropy method is able to provide optimal solution with preferred weights for decision makers who has diverse preferences. For instance, government workers could be more interested in how water supply meets for water users, water companies prefer least-cost solutions, while environmental protection agencies would like to minimize the influence on the environment. The comparison between r-MQSFLA and MOSFLA on the five-performance metrics argues that the approach can offer better solutions for IBWT.

The three scenarios used in this study provide a useful guide for future IBWT under uncertainty. When considering multiple scenarios, we should not expect to find a universal solution that is optimal under all scenarios, especially when there are conflicting objectives (Tian et al., 2017a). This study shows variations in system performance when experiencing different natural inflow and water demands in a water transfer system, through different pathways of pumping stations, sluices and lakes. In addition, an IBWT project across regional, and local bound might be operated when a basin suffers drought or water shortage. This study performs well in fulfilling natural water resources utilization on a monthly time step for different hydrological (normal, dry, and extremely dry) years, which offers a baseline for a potential water transfer. Especially for the extremely dry scenario, it shows how the water transfer project helps to secure water supply with a low inflow and high demand.

6 Conclusions

IBWT are effective engineering countermeasures that can be taken to improve the inter-basin water resource sustainable development and balance the uneven distribution of water resources. This study proposed an integrated many-objective optimization approach involving many-objective optimization model, MOEAs, and MCDM to water resources allocation for

IBWT under various scenarios. The approach included three parts: (1) formulating a many-objective optimization problem (2) employing the r-MQSFLA to solve the optimization problem; (3) utilizing the AHP-Entropy method to filter the Pareto solutions derived by the r-MQSFLA. Here, the AHP-Entropy method applied to select the preferred solution from Pareto sets could combine subjective and objective analysis for stakeholders who have diverse preferences.

In r-MQSFLA, the real-coded quantum computer and ExA with dynamic updating mechanism were applied to SFLA aiming to improve the diversity and convergence of Pareto solutions. The performance of r-MQSFLA was tested with that of NSGA-II, SPEA-II, ε-MOEA, IBEA, MOEA/D, and MOSFLA in solving five benchmark problems (ZDT1, ZDT2, ZDT3, ZDT4, and ZDT6). The indictors of convergence and diversity for the five benchmark problems indicated that r-MQSFLA inspired from a real-coded quantum computer could strength the search ability of SFLA, while the ExA with dynamic updating mechanism could improve the diversity of Pareto solutions.

The many-objective approach was then applied to optimize water transfers of JE-SNWT Project under normal, dry, and extremely dry scenarios. The performance of r-MQSFLA was also tested with that of the six algorithms in solving three JE-SNWT problems. r-MQSFLA displayed approximate performance with SPEA2, ε-MOEA, and NSGA-II and its performance was improved significantly than MOSFLA in terms of convergence and diversity. Overall, the preferred solutions selected by the AHP-Entropy method with r-MQSFLA performed well in fulfilling natural water resources utilization on a monthly time step to get out of a tremendous drought condition through sacrificing economic cost.

This study has proved the efficiency and usefulness of the proposed many-objective optimization methodology for obtaining water allocation guidelines to policymakers for IBWT under different scenarios. However, the formulation and scenarios used here can not completely represent the real-word problems. The further study will explore more realistic decisions with unknown inflows under uncertainty (Giuliani et al., 2016; Quinn et al., 2017).

Acknowledgments

This research is funded by the Water Conservancy Science and Technology Project of Jiangsu Province (2014012). The Water Resources Department of Jiangsu Province is greatly acknowledged for providing the data relevant to the Eastern Route of South-to-North Water Transfer Project used in this study. Editors and reviewers are greatly acknowledged for providing very useful comments to improve the quality of our manuscript.

References

Ahandani, M. A., Alavi-Rad, H. 2015. Opposition-based learning in shuffled frog leaping: An application for parameter identification. Information sciences, 291, 19-42.

Akron, A., Ghermandi, A., Dayan, T., Hershkovitz, Y. 2017. Interbasin water transfer for the rehabilitation of a transboundary Mediterranean stream: An economic analysis. Journal of environmental management, 202, 276-286.

Al-Aomar, R. 2010. A combined ahp-entropy method for deriving subjective and objective criteria weights. International Journal of Industrial Engineering: theory, applications and practice, 17(1), 12-24.

Arpaia, P., Maisto, D., Manna, C. 2011. A Quantum-inspired Evolutionary Algorithm with a competitive variation operator for Multiple-Fault Diagnosis. Applied Soft Computing, 11(8), 4655-4666.

Aşchilean, I., Badea, G., Giurca, I., Naghiu, G. S., Iloaie, F. G. 2017. Choosing the Optimal Technology to Rehabilitate the Pipes in Water Distribution Systems Using the AHP Method. Energy Procedia, 112, 19-26.

Bai, H., Zheng, J., Yu, G., Yang, S., Zou, J. 2019. A Pareto-based many-objective evolutionary algorithm using space partitioning selection and angle-based truncation. Information sciences, 478, 186-207.

Beume, N., Naujoks, B., Emmerich, M. 2007. SMS-EMOA: Multiobjective selection based on dominated hypervolume. European Journal of Operational Research, 181(3), 1653-1669.

Bleuler, S., Brack, M., Thiele, L., Zitzler, E. 2001. Multiobjective genetic programming: reducing bloat using SPEA2. Paper presented at the Proceedings of the 2001 Congress on Evolutionary Computation.

Chen, J.-F., Hsieh, H.-N., Do, Q. H. 2015. Evaluating teaching performance based on fuzzy AHP and comprehensive evaluation approach. Applied Soft Computing, 28, 100-108.

Chen, X., Yang, G., Huang, M. 2013. Real-coded quantum differential evolution algorithm. Journal of Chinese Computer Systems, 34(5), 1141-1146.

Cheng, R., Jin, Y., Olhofer, M., Sendhoff, B. 2016. A Reference Vector Guided Evolutionary Algorithm for Many-Objective Optimization. IEEE transactions on evolutionary computation, 20(5), 773-791.

Deb, K., Jain, S. 2002. Running performance metrics for evolutionary multi-objective optimization. Proceedings of the 4th Asia-Pacific Conference on Simulated Evolution and Learning, 13-20.

Deb, K., Mohan, M., Mishra, S. 2003. A fast multi-objective evolutionary algorithm for finding well-spread pareto-optimal solutions. KanGAL report, 2003002.

Deb, K., Mohan, M., Mishra, S. 2005. Evaluating the ε-Domination Based Multi-Objective Evolutionary Algorithm for a Quick Computation of Pareto-Optimal Solutions. Evolutionary Computation, 13(4), 501-525.

Deb, K., Pratap, A., Agarwal, S., Meyarivan, T. 2002. A fast and elitist multiobjective genetic algorithm: NSGA-II. IEEE transactions on evolutionary computation, 6(2), 182-197.

Elbeltagi, E., Hegazy, T., Grierson, D. 2007. A modified shuffled frog-leaping optimization algorithm: applications to project management. Structure and Infrastructure Engineering, 3(1), 53-60.

Eusuff, M., Lansey, K., Pasha, F. 2006. Shuffled frog-leaping algorithm: a memetic meta-heuristic for discrete optimization. Engineering optimization, 38(2), 129-154.

Fang, G., Guo, Y., Wen, X., Fu, X., Lei, X., Tian, Y. 2018a. Multi-Objective Differential Evolution-Chaos Shuffled Frog Leaping Algorithm for Water Resources System Optimization. Water Resources Management, 32(12), 3835-3852.

Fang, G., Guo, Y., Wen, X., Huang, X. 2018b. Appliacation of improved multi-objective quantum genetic algorithm on water resources optimal operation of Jiangsu Section of South-to-North Water Transfer East Route Project. Water Resources Protection, 34(2), 34-41.

Fonseca, C. M., Fleming, P. J., Zitzler, E., Deb, K., Thiele, L. 2003. Evolutionary multi-criterion optimization. Paper presented at the Second International Conference, EMO 2003.

Gallardo, B., Aldridge, D. C. 2018. Inter-basin water transfers and the expansion of aquatic invasive species. Water Research, 143, 282-291.

Gao, H., Cao, J. 2012. Membrane-inspired quantum shuffled frog leaping algorithm for spectrum allocation. Journal of Systems Engineering and Electronics, 23(5), 679-688.

Ghimire, L. P., Kim, Y. 2018. An analysis on barriers to renewable energy development in the context of Nepal using AHP. Renewable Energy, 129, 446-456.

Giuliani, M., Castelletti, A., Pianosi, F., Mason, E., Reed, P. M. 2016. Curses, Tradeoffs, and Scalable Management: Advancing Evolutionary Multiobjective Direct Policy Search to

Improve Water Reservoir Operations. Journal of Water Resources Planning & Management, 142(2), 04015050.

Hidalgo-Paniagua, A., Vega-Rodríguez, M. A., Ferruz, J., Pavón, N. 2015. MOSFLA-MRPP: Multi-Objective Shuffled Frog-Leaping Algorithm applied to Mobile Robot Path Planning. Engineering Applications of Artificial Intelligence, 44, 123-136.

Hua, S., Ling, B. 2010. The fuzzy integrative evaluation model and empirical study of enterprise strategy risk based on AHP-entropy combination weight method. Paper presented at the Management Science and Engineering (ICMSE), 2010 International Conference on.

Jain, S. K., Reddy, N. S. R. K., Chaube, U. C. 2005. Analysis of a large inter-basin water transfer system in India / Analyse d'un grand système de transfert d'eau inter-bassins en Inde. Hydrological Sciences Journal, 50(1), 125-137.

Jeuland, M., Hansen, K., Doherty, H., Eastman, L. B., Tchamkina, M. 2019. The economic impacts of water information systems: A systematic review. Water Resources and Economics, 26, 100128.

Jiao, L., Li, Y., Gong, M., Zhang, X. 2008. Quantum-Inspired Immune Clonal Algorithm for Global Optimization. IEEE Transactions on Systems, Man, and Cybernetics, Part B (Cybernetics), 38(5), 1234-1253.

Kasprzyk, J. R., Reed, P. M., Characklis, G. W., Kirsch, B. R. 2012. Many-objective de Novo water supply portfolio planning under deep uncertainty. Environmental Modelling & Software, 34, 87-104.

Kirar, J. S., Agrawal, R. K. 2019. A combination of spectral graph theory and quantum genetic algorithm to find relevant set of electrodes for motor imagery classification. Applied Soft Computing, 105519.

Kollat, J. B., Reed, P. 2007. A framework for Visually Interactive Decision-making and Design using Evolutionary Multi-objective Optimization (VIDEO). Environmental Modelling & Software, 22(12), 1691-1704.

Kollat, J. B., Reed, P. M., Maxwell, R. 2011. Many- objective groundwater monitoring network design using bias- aware ensemble Kalman filtering, evolutionary optimization, and visual analytics. Water Resources Research, 47(2), 155-170.

Lamboia, F., de Arruda, L. V. R., Neves, F. 2016. Modified Shuffled Frog Leaping Algorithm for Improved Pareto-Set Computation: Application to Product Transport in Pipeline Networks. Journal of Control, Automation and Electrical Systems, 27(1), 43-59.

Lasserre, F. 2017. Water exportation projects in Quebec : Rise andfall of a national development lever. Hérodote, 2017(165), 143-164.

Li, Y. H., Zhou, J. Z., Zhang, Y. C., Qin, H., Liu, L. 2010. Novel multiobjective shuffled frog leaping algorithm with application to reservoir flood control operation. Journal of Water Resources Planning & Management, 136(2), 217-226.

Liu, G., Chen, L., Shen, Z., Xiao, Y., Wei, G. 2019. A fast and robust simulation-optimization methodology for stormwater quality management. Journal of Hydrology, 576, 520-527.

Lopez, J. C. 2018. Interbasin water transfers and the size of regions: An economic geography example. Water Resources and Economics, 21, 40-54.

Madani, K., Lund, J. R. 2011. A Monte-Carlo game theoretic approach for Multi-Criteria Decision Making under uncertainty. Advances in water resources, 34(5), 607-616.

Matete, M., Hassan, R. 2006. Integrated ecological economics accounting approach to evaluation of inter-basin water transfers: An application to the Lesotho Highlands Water Project. Ecological Economics, 60(1), 246-259.

Modiri-Delshad, M., Rahim, N. A. 2016. Multi-objective backtracking search algorithm for economic emission dispatch problem. Applied Soft Computing, 40, 479-494.

Nouiri, I. 2014. Multi-Objective tool to optimize the Water Resources Management using Genetic Algorithm and the Pareto Optimality Concept. Water Resources Management, 28(10), 2885-2901.

Orouji, H., Haddad, O. B., Fallah-Mehdipour, E., Mariño, M. 2013. Extraction of decision alternatives in project management: Application of hybrid PSO-SFLA. Journal of Management in Engineering, 30(1), 50-59.

Perolat, J., Couso, I., Loquin, K., Strauss, O. 2015. Generalizing the Wilcoxon rank-sum test for interval data. International Journal of Approximate Reasoning, 56, 108-121.

Pohlner, H. 2016. Institutional change and the political economy of water megaprojects: China's south-north water transfer. Global environmental change, 38, 205-216.

Quinn, J. D., Reed, P. M., Keller, K. 2017. Direct policy search for robust multi-objective management of deeply uncertain socio-ecological tipping points. Environmental Modelling & Software, 92, 125-141.

Reed, P. M., Hadka, D., Herman, J. D., Kasprzyk, J. R., Kollat, J. B. 2013. Evolutionary multiobjective optimization in water resources: The past, present, and future. Advances in water resources, 51, 438-456.

Reed, P. M., Kollat, J. B. 2013. Visual analytics clarify the scalability and effectiveness of massively parallel many-objective optimization: A groundwater monitoring design example. Advances in water resources, 56, 1-13.

Ren, C., Li, Z., Zhang, H. 2019. Integrated multi-objective stochastic fuzzy programming and AHP method for agricultural water and land optimization allocation under multiple uncertainties. Journal of Cleaner Production, 210, 12-24.

Ridolfi, E., Rianna, M., Trani, G., Alfonso, L., Di Baldassarre, G., Napolitano, F., et al. 2016. A new methodology to define homogeneous regions through an entropy based clustering method. Advances in water resources, 96, 237-250.

Sadegh, M., Mahjouri, N., Kerachian, R. 2010. Optimal Inter-Basin Water Allocation Using Crisp and Fuzzy Shapley Games. Water Resources Management, 24(10), 2291-2310.

Tang, C., Yi, Y., Yang, Z., Cheng, X. 2014. Water pollution risk simulation and prediction in the main canal of the South-to-North Water Transfer Project. Journal of Hydrology, 519, 2111-2120.

Tian, X., Guo, Y., Negenborn, R. R., Wei, L., Lin, N. M., Maestre, J. M. 2019. Multi-Scenario Model Predictive Control Based on Genetic Algorithms for Level Regulation of Open Water Systems under Ensemble Forecasts. Water Resources Management, 33(9), 3025-3040.

Tian, X., Negenborn, R. R., van Overloop, P.-J., Maestre, J. M., Sadowska, A., van de Giesen, N. 2017a. Efficient multi-scenario Model Predictive Control for water resources management with ensemble streamflow forecasts. Advances in water resources, 109, 58-68.

Tian, Y., Cheng, R., Zhang, X., Jin, Y. 2017b. PlatEMO: A MATLAB Platform for Evolutionary Multi-Objective Optimization. IEEE Computational Intelligence Magazine, 12, 73-87.

Vlachogiannis, J. G., Lee, K. Y. 2008. Quantum-Inspired Evolutionary Algorithm for Real and Reactive Power Dispatch. IEEE Transactions on Power Systems, 23(4), 1627-1636.

Vogel, R. M., Lall, U., Cai, X., Rajagopalan, B., Weiskel, P. K., Hooper, R. P., et al. 2015. Hydrology: The interdisciplinary science of water. Water Resources Research, 51(6), 4409-4430.

Wang, J., Diao, M., Yue, K. 2017. Optimization on pinch point temperature difference of ORC system based on AHP-Entropy method. Energy, 141, 97-107.

Wang, P., Fang, G., Guo, Y., Wen, X. 2016. Research on Water Resources Optimal Scheduling Based on Improved Quantum Genetic Algorithm. Journal of China Three Gorges University, 38(5), 7-13.

Wang, X., Li, Q., Yin, J., Han, X., Hao, W. 2019. An Adaptive Denoising and Detection Approach for Underwater Sonar Image. Remote Sensing, 11(4), 396.

Xiang, Y., Zhou, Y. 2015. A dynamic multi-colony artificial bee colony algorithm for multi-objective optimization. Applied Soft Computing, 35, 766-785.

Yan, B., Chen, L. 2013. Coincidence probability of precipitation for the middle route of South-to-North water transfer project in China. Journal of Hydrology, 499, 19-26.

Yang, G., Guo, S., Li, L., Hong, X., Wang, L. 2016. Multi-objective operating rules for Danjiangkou reservoir under climate change. Water Resources Management, 30(3), 1183-1202.

Yang, Y., Luo, J., Huang, L., Liu, Q. 2018. A many-objective evolutionary algorithm with epsilon-indicator direction vector. Applied Soft Computing, 76, 326-355.

Yong, P., Chu, J., Peng, A., Zhou, H. 2015. Optimization Operation Model Coupled with Improving Water-Transfer Rules and Hedging Rules for Inter-Basin Water Transfer-Supply Systems. Water Resources Management, 29(10), 3787-3806.

Zahmatkesh, Z., Karamouz, M., Nazif, S. 2015. Uncertainty based modeling of rainfall-runoff: Combined differential evolution adaptive Metropolis (DREAM) and K-means clustering. Advances in water resources, 83, 405-420.

Zeff, H. B., Kasprzyk, J. R., Herman, J. D., Reed, P. M., Characklis, G. W. 2014. Navigating financial and supply reliability tradeoffs in regional drought management portfolios. Water Resources Research, 50(6), 4906-4923.

Zhang, C., Li, Y., Chu, J., Fu, G., Tang, R., Qi, W. 2017. Use of Many-Objective Visual Analytics to Analyze Water Supply Objective Trade-Offs with Water Transfer. Journal of Water Resources Planning and Management, 143(8), 05017006.

Zhang, Q., Liu, W., Li, H. 2009. The Performance of a New Version of MOEA/D. The 11th conference on Congress on Evolutionary Computation.

Zhou, Y., Guo, S., Hong, X., Chang, F.-J. 2017. Systematic impact assessment on inter-basin water transfer projects of the Hanjiang River Basin in China. Journal of Hydrology, 553, 584-595.

Zhou, Y., Guo, S., Xu, C.-Y., Liu, D., Chen, L., Wang, D. 2015. Integrated optimal allocation model for complex adaptive system of water resources management (II): Case study. Journal of Hydrology, 531, 977-991.

Zhuang, W., Ying, S. C., Frie, A. L., Wang, Q., Song, J., Liu, Y., et al. 2019. Distribution, pollution status, and source apportionment of trace metals in lake sediments under the influence of the South-to-North Water Transfer Project, China. Science of the Total Environment, 671, 108-118.

Zitzler, E., Künzli, S. 2004. Indicator-Based Selection in Multiobjective Search. The 8th International Conference on Parallel Problem Solving from Nature.

Zitzler, E., Thiele, L., Laumanns, M., Fonseca, C. M., Fonseca, V. G. D. 2003. Performance Assessment of Multiobjective Optimizers: An Analysis and Review. IEEE transactions on evolutionary computation, 7(2), 117-132.